

Supporting information

High Efficient Electrochemical Hydrodeoxygenation of Bio-Phenols to Hydrocarbon Fuels by Superacid-Nobel Metal Particle Dual-Catalyst System

Wei Liu, Wenqin You, Yutao Gong and Yulin Deng*

School of Chemical & Biomolecular Engineering and RBI, Georgia Institute of Technology, 500
10th Street N.W., Atlanta, GA 30332, USA

*Corresponding author. E-mail: yulin.deng@rbi.gatech.edu

Contents:

Materials and supplementary methods

Materials

Cyclic voltammogram

Supporting Figures (Figure S1 ~ S15)

Supporting Table (Table S1 ~ S5)

Supporting Text

1. *Electron and proton transfer between anode and cathode compartment during the electrolysis*
2. *Chemical analysis of products using Gas chromatography (GC)*
3. *Studies of Phenol consuming in the electrolysis*
4. *Turnover rates investigation*
5. *DFT calculation of electro-hydrogenation-and-hydrodeoxygenation routes*
 - a. *Phenol hydrogenation and hydrodeoxygenation*
 - b. *Hydrodeoxygenation of cyclohexanol*

Materials and supplementary methods

Materials

Silicotungstic acid ($\text{H}_4\text{SiW}_{12}\text{O}_{40}$ noted as SiW_{12}) was purchased from Alfa Aesar. Pt/C, Pd/C and Rh/C catalysts are 5wt% metal loaded on matrix activated carbon support, which were purchased from Sigma Aldrich. Pt/ Al_2O_3 (platinum on alumina, 5% loading) was purchased from Sigma Aldrich. The organic substrates used in the electrolysis include: 2-butanone (Sigma Aldrich, >99.0%), phenol (Alfa Aesar, 99.5%), cyclohexanol (Alfa Aesar, >99%), benzyl alcohol (Sigma Aldrich, >99.8%), tert-butyl alcohol (Sigma Aldrich, >99.5%), n-butyl alcohol (Sigma Aldrich, >99.8%), diphenylmethanol (Alfa Aesar, 99%), diphenylmethanone (Sigma Aldrich, >99%), acetylacetone (Sigma Aldrich, >99.3%), 1,3-diphenylpropane-1,3-dione (Sigma Aldrich, >98%), vanillin (Sigma Aldrich, >98%), salicylaldehyde (Sigma Aldrich, >98%), acetovanillone (Sigma Aldrich, >98%), diphenyl ether (Alfa Aesar, 99%), 2-Methoxy-4-methylphenol (Alfa Aesar, 98%), guaiacol (Alfa Aesar, 98%), 4-methylcatechol (Alfa Aesar, 98%), catechol (Alfa Aesar, 98%), p-cresol (Alfa Aesar, 98%), 3-methoxycatechol (Sigma Aldrich, >99%), benzoic acid (Sigma Aldrich, >99.5%), methyl benzoate (Sigma Aldrich, >99%), isoeugenol (Sigma Aldrich, >98%). The solvents methanol (Sigma Aldrich, >99.9%) and dichloromethane (Sigma Aldrich, >99.8%) were used. High purity water with a resistivity of $18.2 \text{ M}\Omega\cdot\text{cm}$, obtained through a Milli-Q water purification system, was used for all experimental procedures.

Cyclic voltammogram

The measurements were taken on Versa Stat 3 electrochemical working station using a BASi Ag/AgCl aqueous reference electrode (with 3 M KCl filling solution), a Pt wire counter electrode and a 3 mm diameter graphite electrode. Electrode potentials were converted to the Normal hydrogen electrode (NHE) scale using the equation $E(\text{NHE})=E(\text{Ag}/\text{AgCl})+0.210 \text{ V}$, where $E(\text{NHE})$ is the potential versus NHE and $E(\text{Ag}/\text{AgCl})$ is the measured potential versus Ag/AgCl.

Supporting Figures (Figure S1 ~ S15)

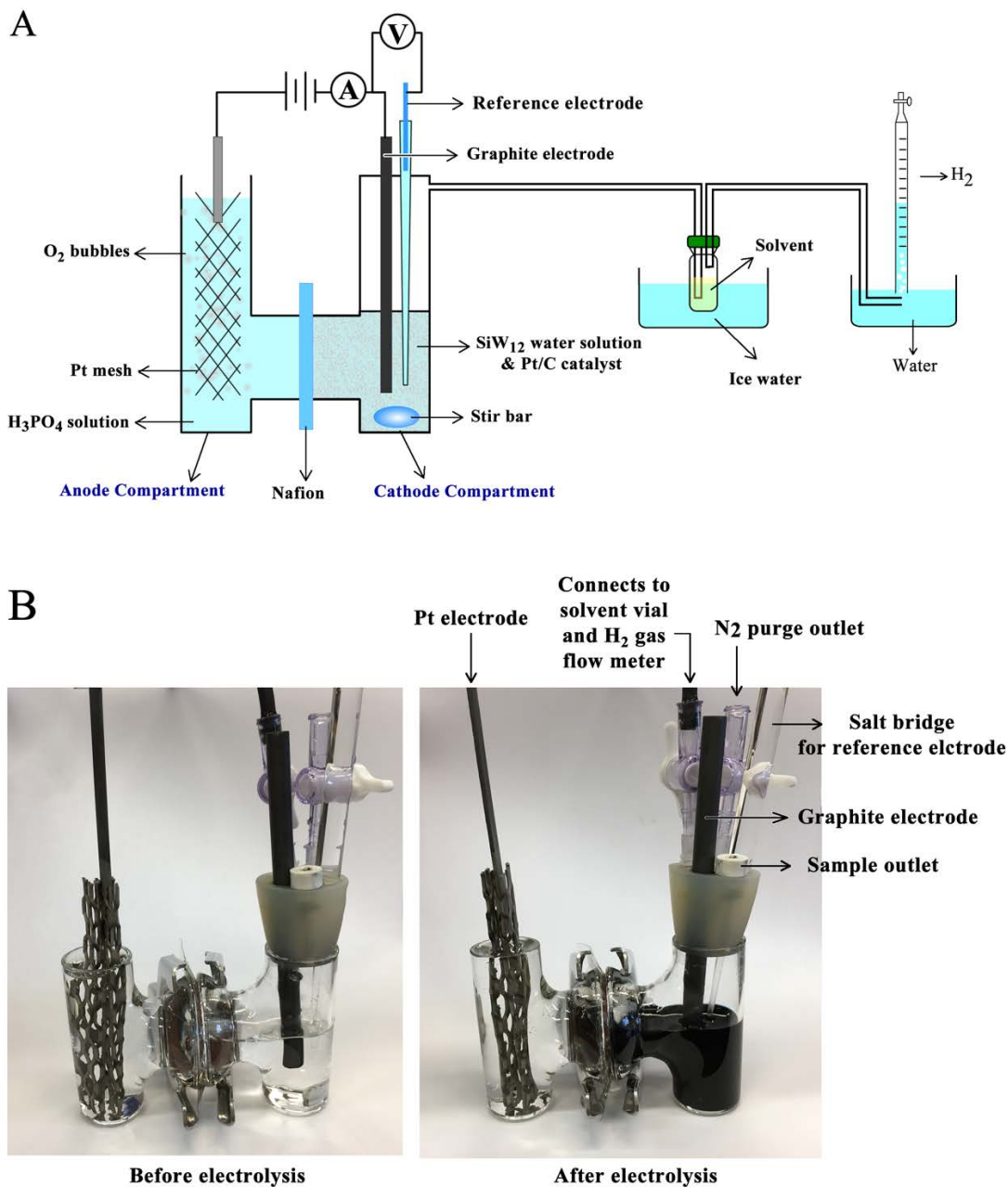


Figure S1 Experiment setup for SiW_{12} mediated electro-hydrogenation. (A) Schematic illustration for the three-electrode system of electro-hydrogenation. (B) Photos of the experimental setup. The SiW_{12} reaction solution in cathode compartment is colorless before electro-reduction, and the color turns to dark blue after electrolysis.

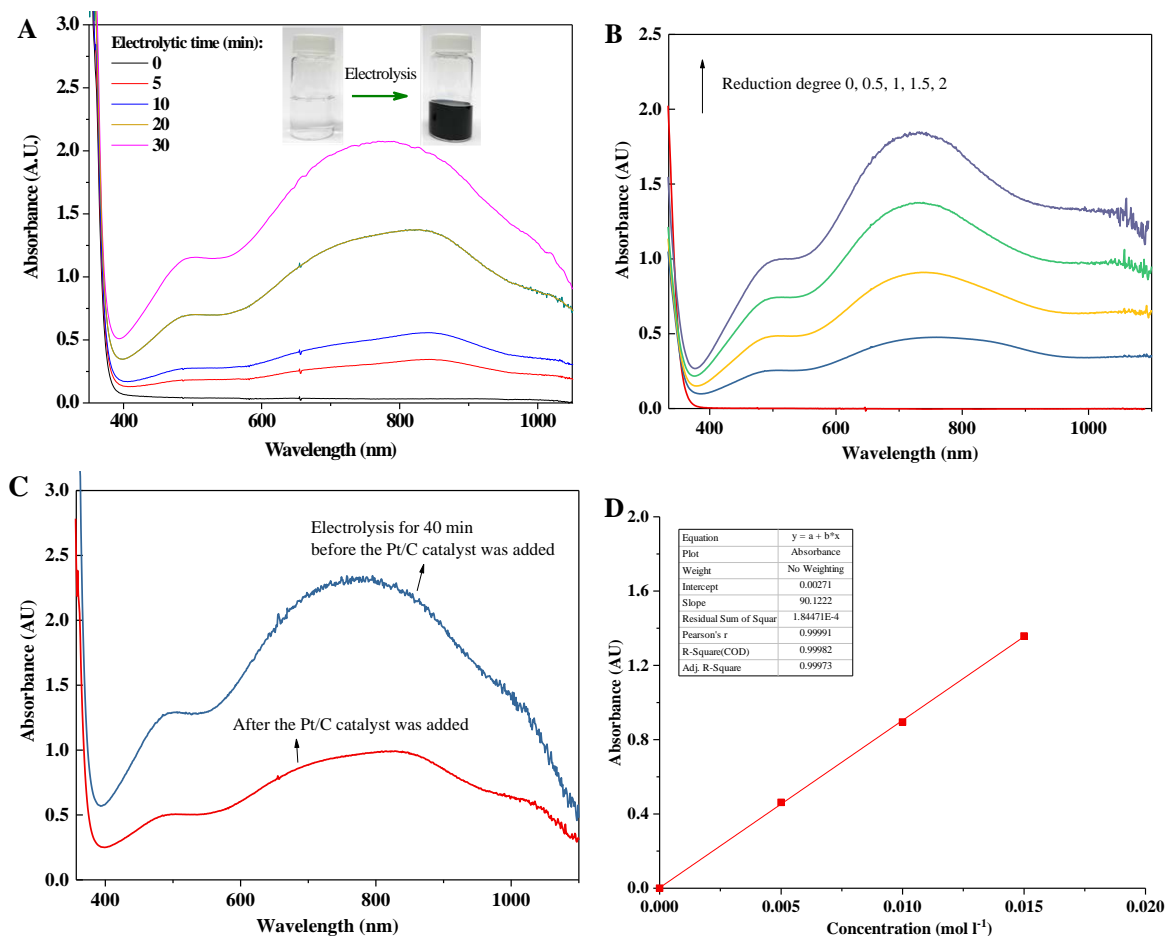


Figure S2 (A) UV-Vis spectra of SiW₁₂ solutions during the electrolysis. The solution was diluted to 10 mmol l⁻¹ for measurement. Inset picture: photographs of SiW₁₂ solution before (colorless) and after electrolytic reduction (dark blue). (B) UV-Vis spectra of SiW₁₂ solutions (10 mmol l⁻¹) with different reduction degrees. (C) UV-Vis spectra of SiW₁₂ solutions before and after adding Pt/C catalyst (diluted to 10 mmol l⁻¹). (D) Absorbance at 700 nm of 1-electron reduced SiW₁₂ solution with different concentrations. Extinction coefficients can be calculated according to the slope 90.1 l mol⁻¹: 90.1/0.05=1802 l mol⁻¹ cm⁻¹ (solution thickness is 0.5 mm in our special cuvette).

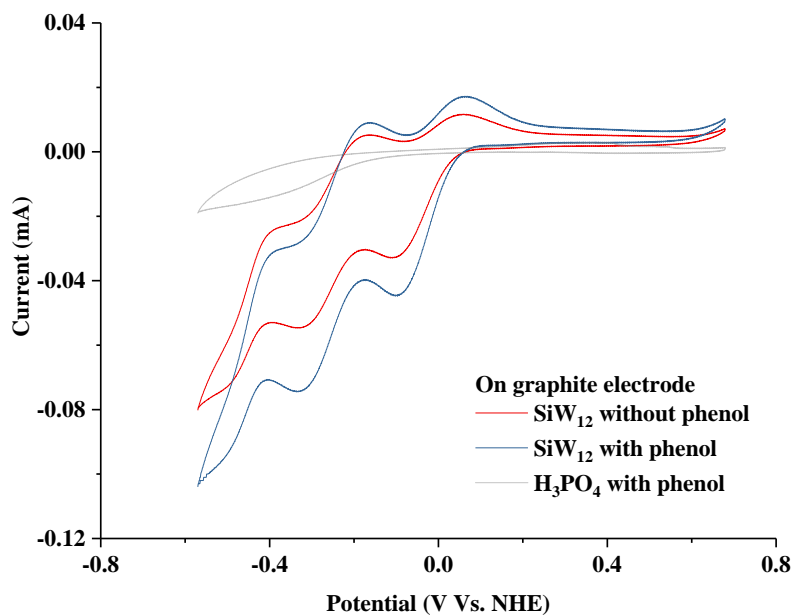


Figure S3 Cyclic voltammogram of reaction solutions (scanning conditions: polished graphite electrode area: 0.3 cm^2 ; concentration of H_3PO_4 or SiW_{12} solution: 10 mmol l^{-1} ; phenol concentration: 10 mmol l^{-1} ; temperature: $20 \text{ }^\circ\text{C}$; scanning rate: 100 mV s^{-1}). The curve of SiW_{12} (red line) includes three redox waves: the waves at $+0.01 \text{ V}$ (I), -0.22 V (II) and -0.41 V (III). The first two waves ascribe to two one-electron reduction processes and the third wave is corresponding to a proton associated two-electron reduction¹. The current increases when phenol was added into SiW_{12} solution but no obvious changes in CV curve, indicating there is no obvious interaction between phenol and SiW_{12} in water solution.

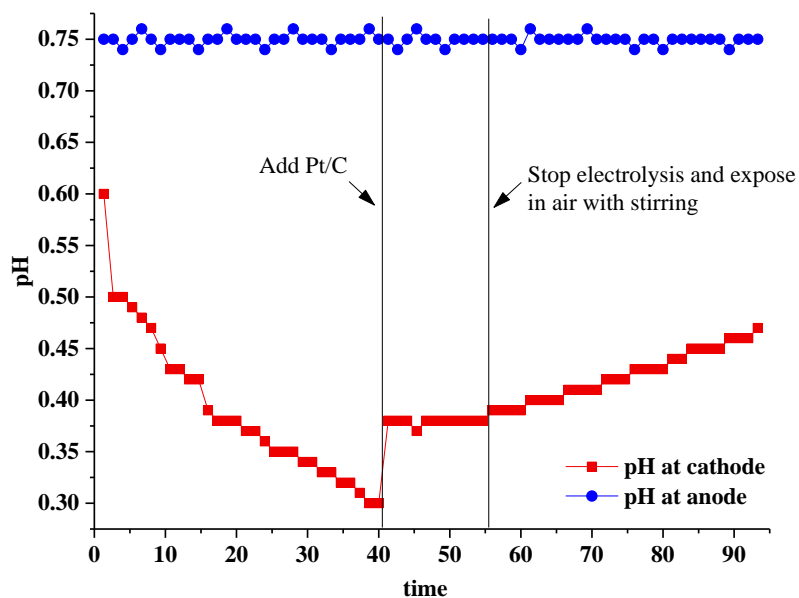


Figure S4 pH changes in electrolyte solution at cathode and anode. During the time from initial to 40 min, the cathode electrolyte was SiW_{12} solution without Pt/C catalyst under the electrolysis at 100 mA cm^{-2} and protection of high pure N_2 atmosphere. At the reaction time of 40 min, Pt/C catalyst was added into cathode solution and the electrolytic current was maintained at 100 mA cm^{-2} . After the reaction time at 55 min, the electrolysis was stopped, and the cathode solution was exposed in air with stirring. The explanation for the curve is given in supporting Text 1.

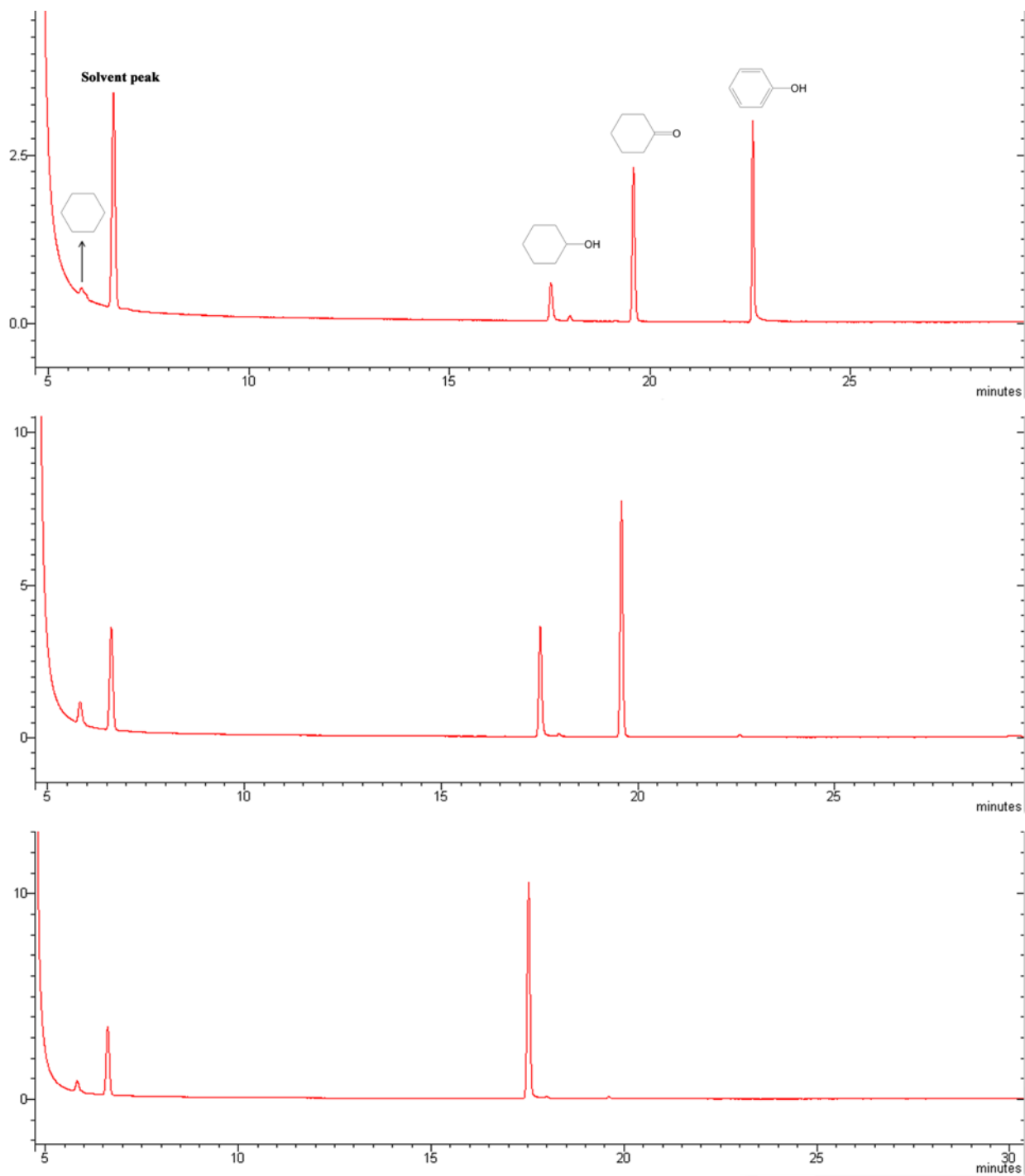


Figure S5 GC-MS analysis of phenol hydrogenation products (experiment entry 4; reaction conditions: 35 °C, 100 mA cm⁻², Pt 5wt%/C 0.013 g, phenol 0.2 mmol; reaction time: 2.9, 16.8 and 18.6 min from top to bottom).

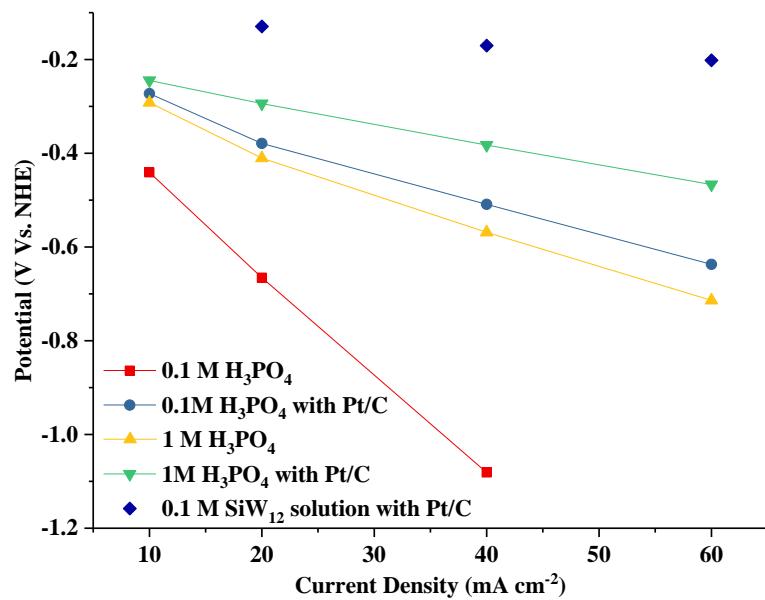


Figure S6 Comparison of the working potential of H₃PO₄ (1 and 0.1 mol l⁻¹) and SiW₁₂ solution under different electrolytic current density.

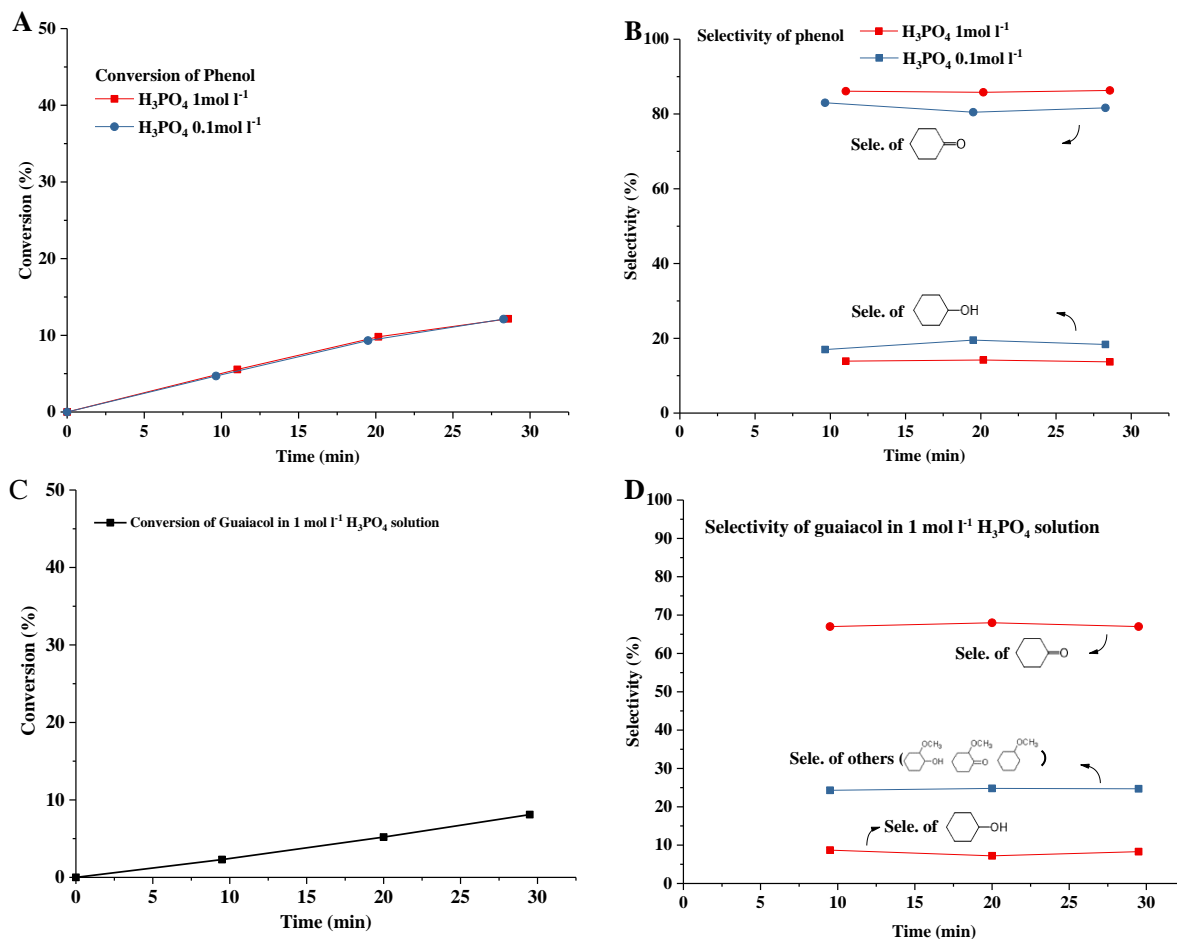


Figure S7 Electric hydrogenation of phenol and guaiacol in the **H_3PO_4 solution** working as catholyte (without SiW_{12}) under the constant working potential at -0.28 V (Vs. NHE). (A) Conversion of phenol, (B) Products selectivity in the phenol hydrogenation, (C) Conversion of guaiacol, (D) Products selectivity in the guaiacol hydrogenation. The figures correspond to the result of entry 1 and 2 (phenol) in Table S1 and entry 22 (guaiacol) in Table S2.

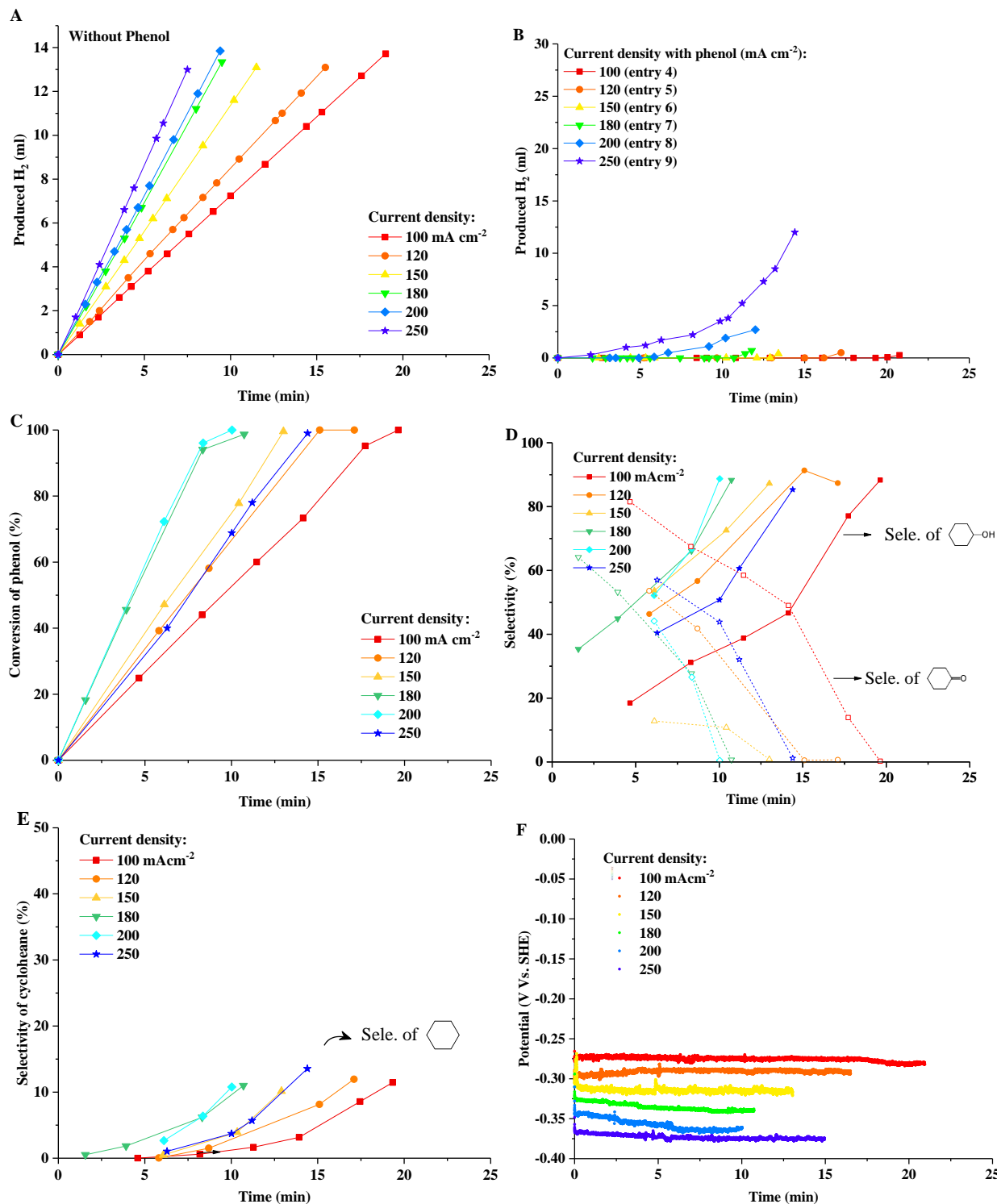


Figure S8 Electro-hydrogenation of phenol in SiW₁₂ and Pt/C reaction system under **different electrolytic current densities** (Entry 4-9 in Table S1). (A) Hydrogen gas production without phenol; (B) Hydrogen gas production with phenol; (C) Conversion of phenol with different current density; (D) Selectivity of cyclohexanol and cyclohexanone; (E) Selectivity of cyclohexane; (F) Working potential under different current density.

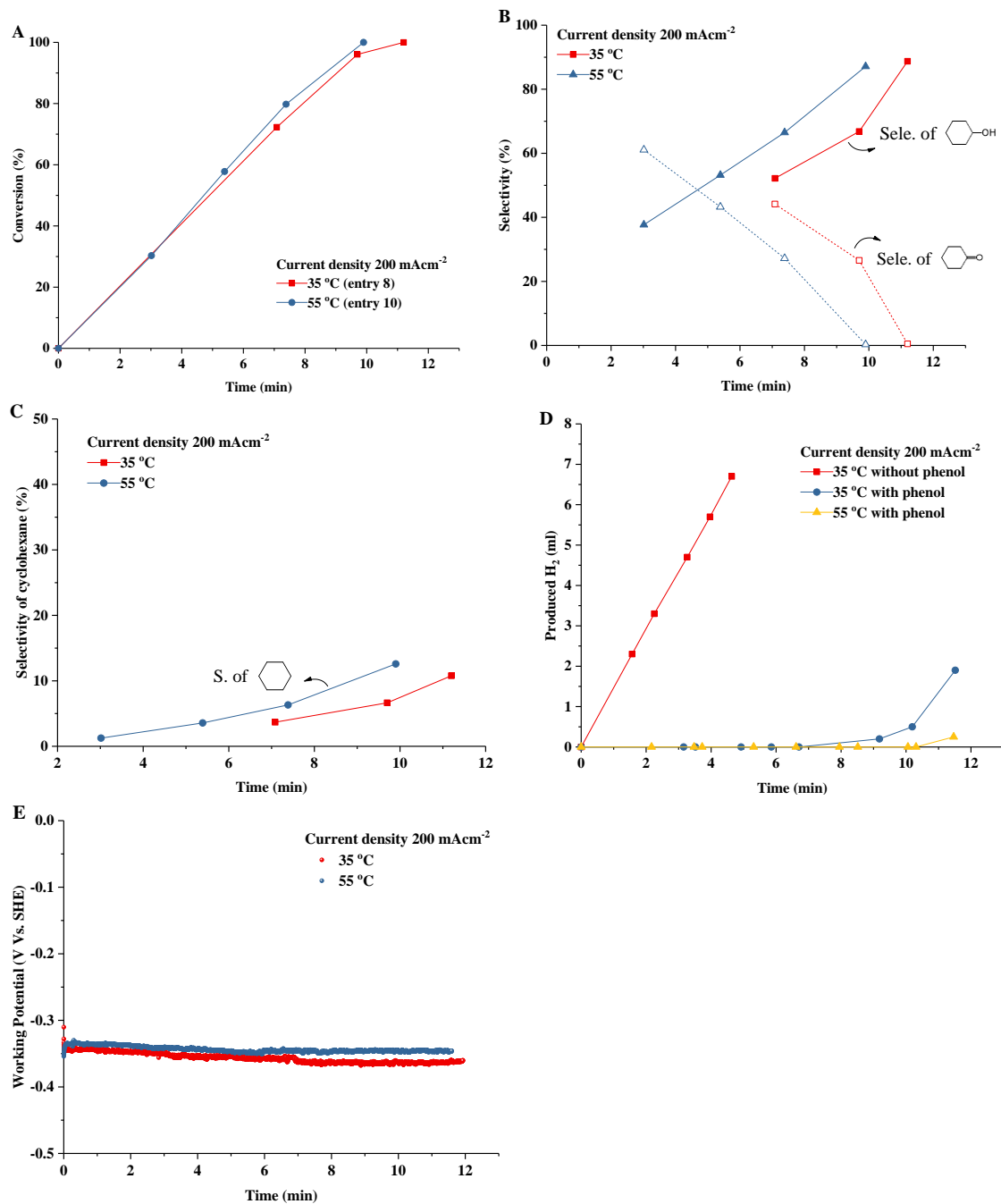


Figure S9 Electro-hydrogenation of phenol under the electrolytic current density of 200 mA cm⁻² with **different reaction temperatures** (Entry 8 and 10 in Table S1). (A) Conversion of phenol with different current density; (B) Selectivity of cyclohexanol and cyclohexanone; (C) Selectivity of cyclohexane; (D) Hydrogen gas production during the electrolysis; (E) Working potential.

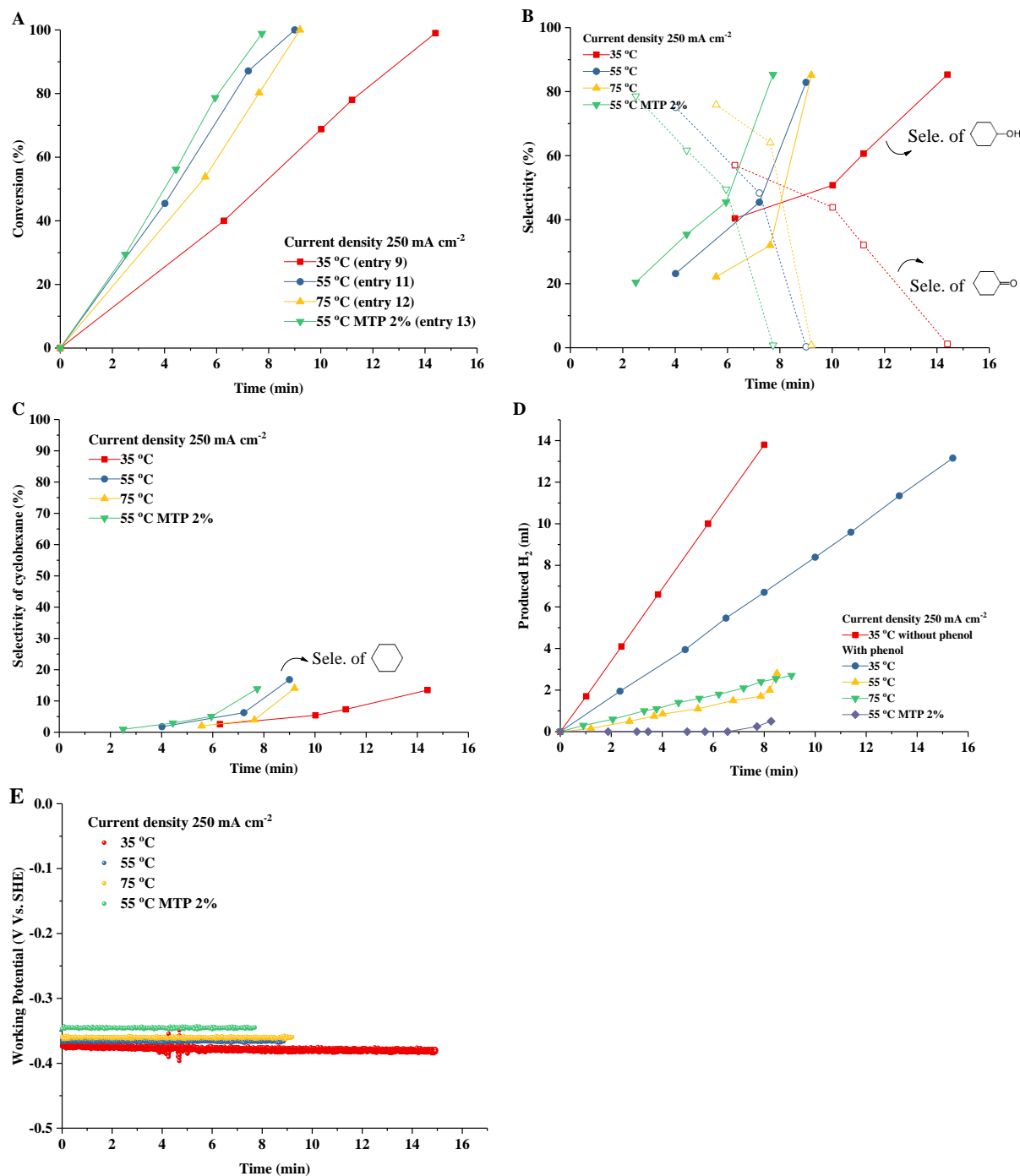


Figure S10 Electro-hydrogenation of phenol under the electrolytic current density of 250 mA cm⁻² with **different reaction temperatures and catalyst additions** (Entry 9, 11, 12 and 13 in Table S1). (A) Conversion of phenol with different current density; (B) Selectivity of cyclohexanol and cyclohexanone; (C) Selectivity of cyclohexane; (D) Hydrogen gas production during the electrolysis; (E) Working potential.

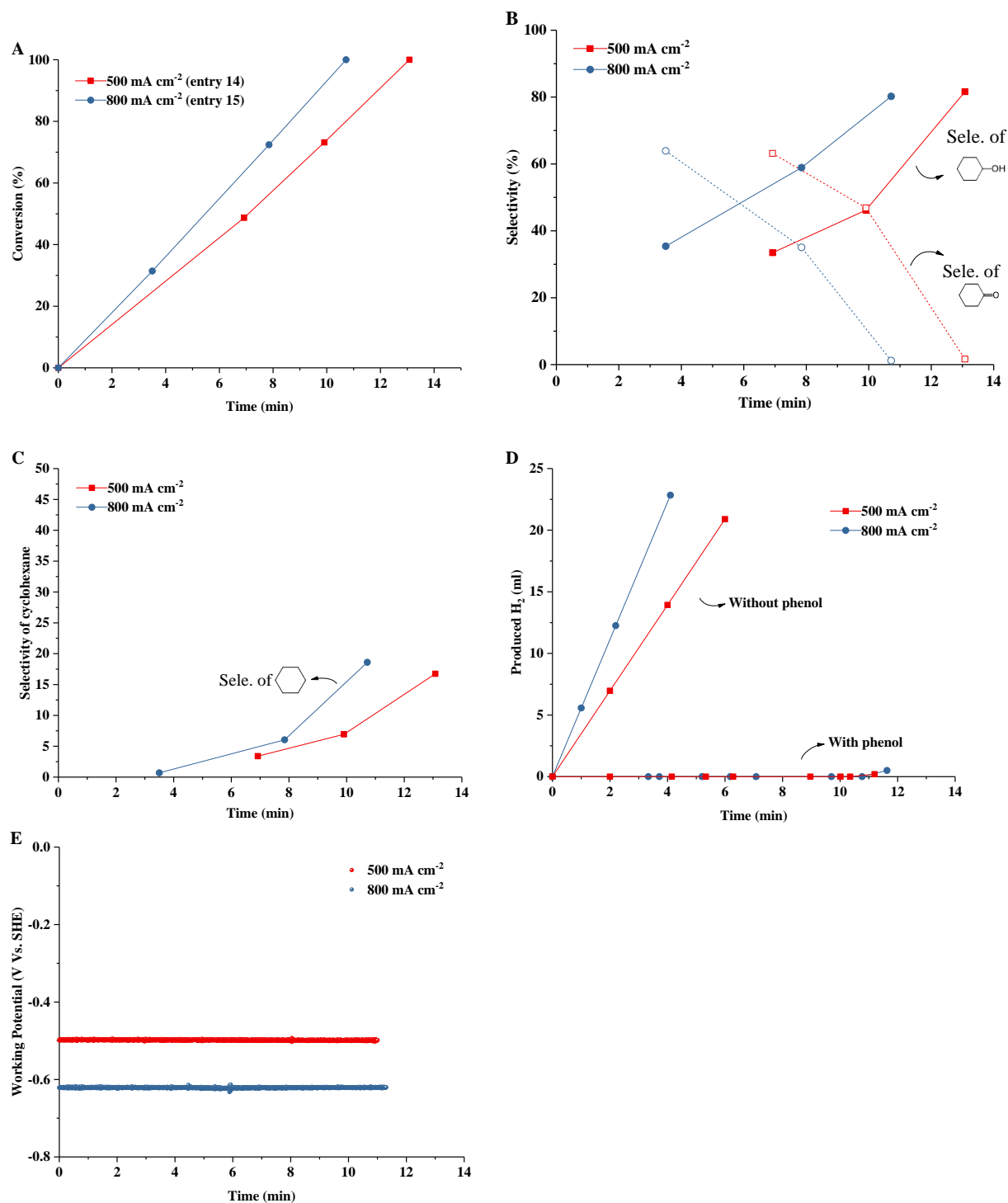


Figure S11 Electro-hydrogenation of phenol under **large current density** of 500 and 800 mA cm⁻² (other conditions are shown in entry 14 and 15 in Table S1). (A) Conversion of phenol with different current density; (B) Selectivity of cyclohexanol and cyclohexanone; (C) Selectivity of cyclohexane; (D) Hydrogen gas production during the electrolysis; (E) Working potential.

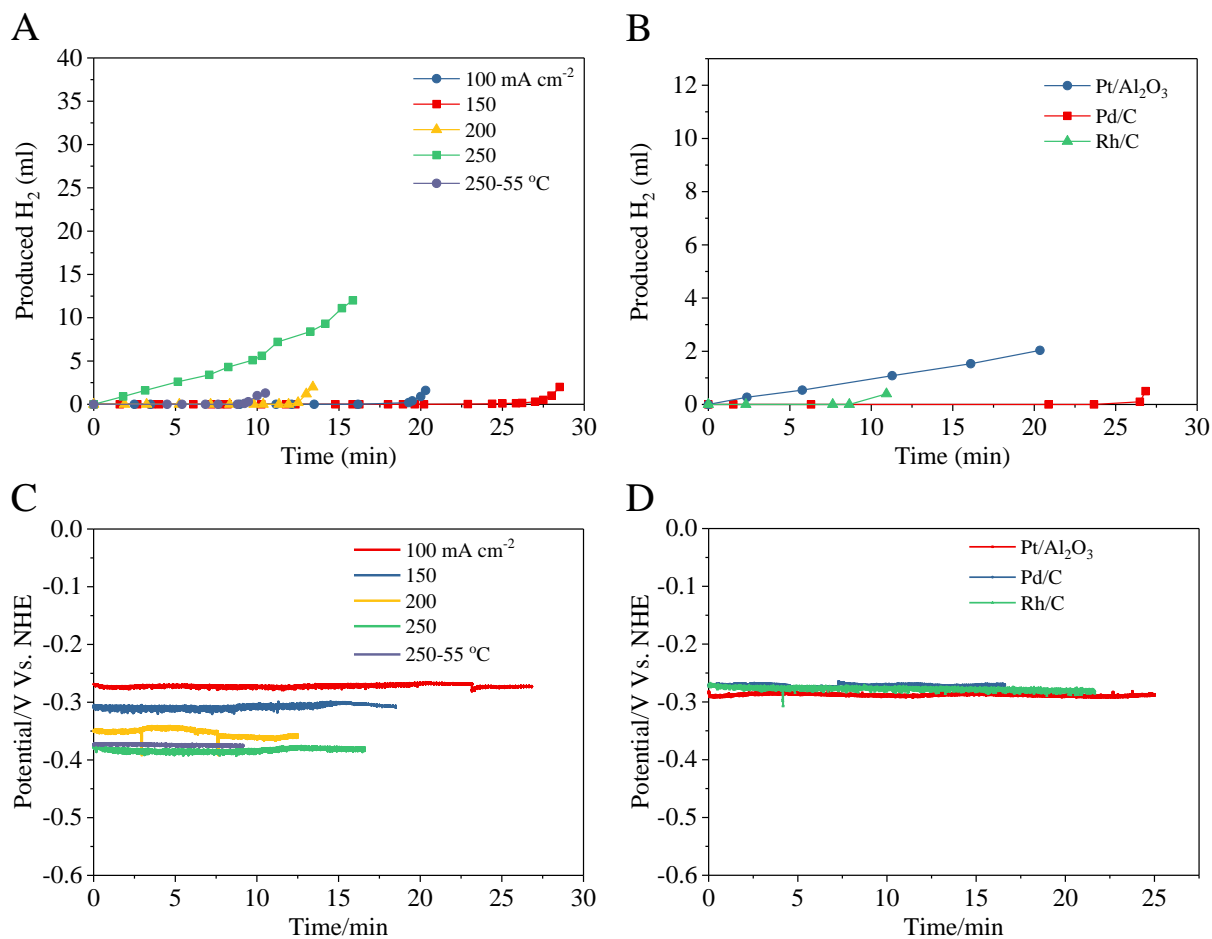


Figure S12 Electro-hydrogenation performances of **guaiacol**. (A) Hydrogen gas production during the electrolysis of guaiacol under different current densities; (B) Hydrogen gas production under different catalysts; (C) Electrolytic potentials during the electrolysis of guaiacol under different current densities; (D) Electrolytic potentials under different catalysts. Product selectivity data are shown in Table S2.

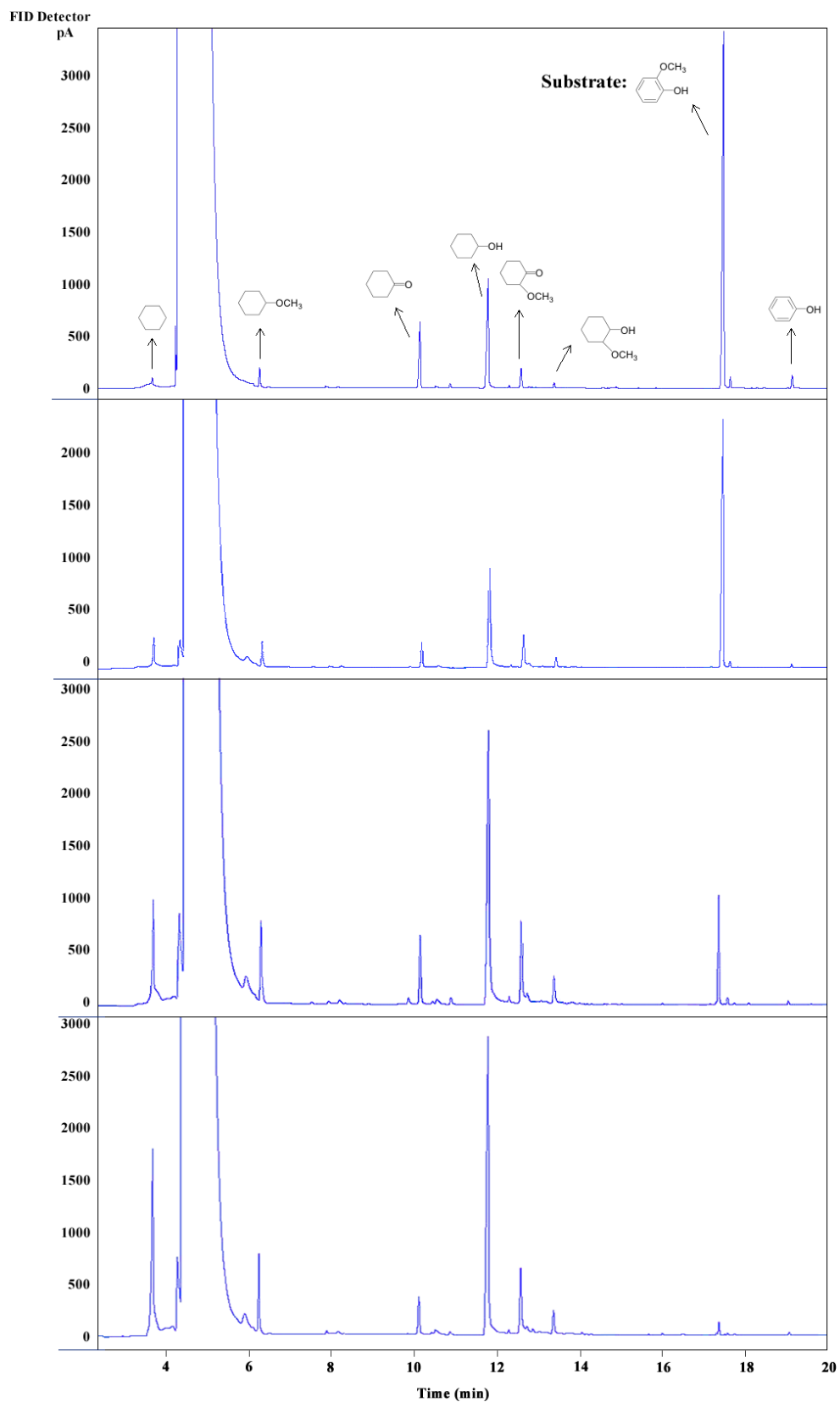


Figure S13 The gas chromatography results of electrolysis of guaiacol at the reaction time of 8.2, 13.3, 20.2 and 25 min (from top to bottom) by using a Nukol column (30 m × 0.25 mm).

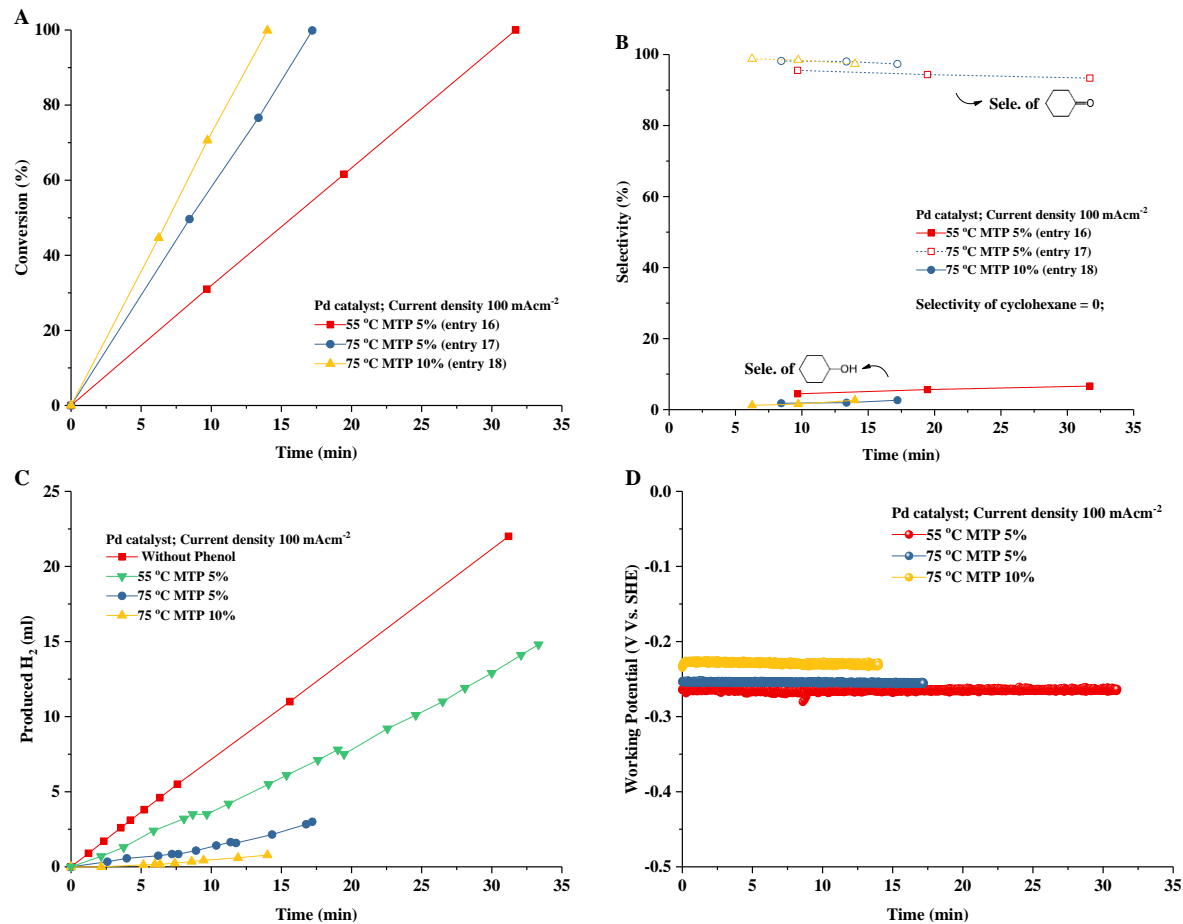


Figure S14 Electro-hydrogenation of phenol over commercial **Pd/C catalyst** (Entry 16 to 18 in Table S1). (A) Conversion of phenol with different current density; (B) Selectivity of cyclohexanol and cyclohexanone; (C) Hydrogen gas production during the electrolysis; (D) Working potential.

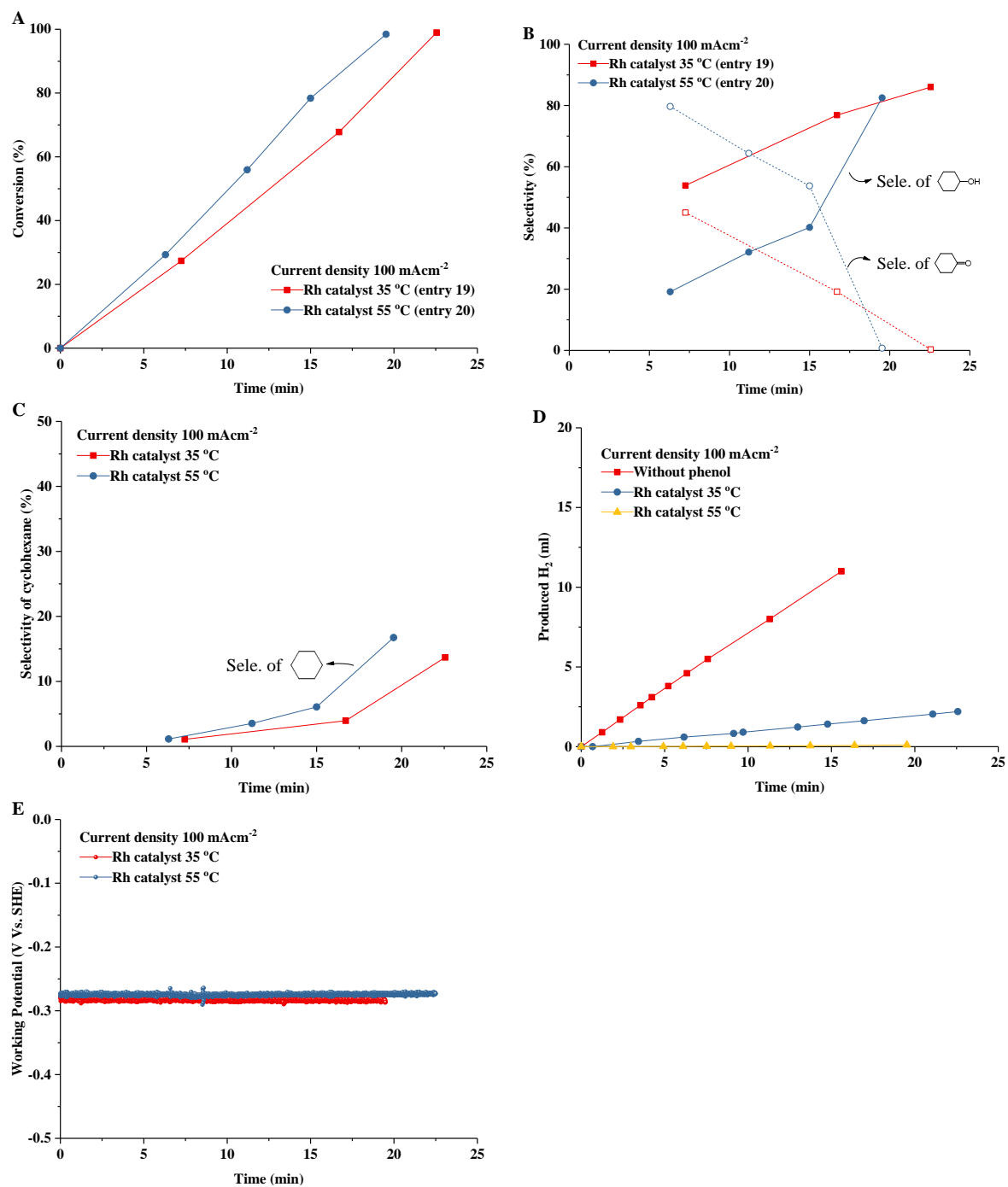
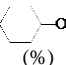
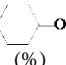
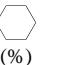


Figure S15 Electro-hydrogenation of phenol over commercial **Rh/C catalyst** (Entry 19 and 20 in Table S1). (A) Conversion of phenol with different current density; (B) Selectivity of cyclohexanol and cyclohexanone; (C) Selectivity of cyclohexane; (D) Hydrogen gas production during the electrolysis; (E) Working potential.

Supporting Table (Table S1 ~ S5)

Table S1 Electro-hydrogenation of phenol over commercial catalysts under different conditions. The catholyte: 10 ml SiW₁₂ (0.1 mol l⁻¹) solution; anolyte: 1 mol l⁻¹ H₃PO₄.

Entry	Phenol (mmol l ⁻¹)	Cat., MTP (%) [*]	T (°C)	I (mA cm ⁻²)	P (V vs. NHE)	Reac. Time (min)	Conv. (%)	Yield of  (%)	Yield of  (%)	Yield of  (%)	F.E. (%)	Rate (mmol g _M ⁻¹ s ⁻¹)	TOF (h ⁻¹)
1 ^{**}	20	Pt/C, 1.7	35	12	-0.272	28.6	12.14	13.7	86.3	0	48.7	0.02	33
2 [†]	20	Pt/C, 1.7	35	14.5	-0.272	28.3	12.1	18.3	81.7	0	41.4	0.02	34
3 [‡]	20	0	35	~0.001	-0.272	30	0	0	0	0	0	0	0
4	20	Pt/C, 1.7	35	100	-0.272	19.3	>99	88.3	0.3	11.4	99	0.28	431
5	20	Pt/C, 1.7	35	120	-0.292	16.1	>99	87.4	0.7	11.9	99	0.34	521
6	20	Pt/C, 1.7	35	150	-0.314	12.9	>99	87.5	1.7	10.8	99	0.43	672
7	20	Pt/C, 1.7	35	180	-0.331	10.7	>99	87.5	1.1	11.3	99	0.54	831
8	20	Pt/C, 1.7	35	200	-0.352	11.2	>99	88.7	0.5	10.7	89.7	0.46	717
9	20	Pt/C, 1.7	35	250	-0.369	14.6	>99	84.8	1.3	13.8	54.0	0.35	540
10	20	Pt/C, 1.7	55	200	-0.342	9.7	>99	87.1	0.3	12.6	99	0.53	815
11	20	Pt/C, 1.7	55	250	-0.361	8.9	>99.9	82.9	0.3	16.8	90.9	0.57	889
12	20	Pt/C, 1.7	75	250	-0.357	9.2	>99.9	85.1	0.8	14.1	87.1	0.55	860
13	20	Pt/C, 2	55	250	-0.359	7.7	>99	84.7	1.2	14.1	99.3	0.55	857
14	56	Pt/C, 1.7	35	500	-0.495	11	>99	81.6	1.6	16.7	98.5	0.45	705
15	89	Pt/C, 1.7	35	800	-0.624	11.3	>99	80.2	1.2	18.6	95.3	0.44	682
16	20	Pd/C , 5	55	100	-0.258	31	99	6.7	93.3	0.0	42.5	0.10	237
17	20	Pd/C , 5	75	100	-0.241	17.2	99	2.7	97.3	0.0	75.1	0.18	427
18	20	Pd/C , 10	75	100	-0.240	14	99	4.5	95.5	0.0	93.0	0.11	262
19	20	Rh/C , 1.7	35	100	-0.274	22.5	99	85.5	0.7	13.9	87.1	0.14	153
20	20	Rh/C , 1.7	55	100	-0.259	19.5	99	81.7	1.2	17.0	99.7	0.16	177
21	20	Pt/ Al₂O₃ , 1.7	55	100	-0.301	20.8	99	83.7	2.6	13.6	95.1	0.25	-
22 ^{††}	20	Pt/C, 1.7	35	44	-0.272	28.5	51.4	83.7	2.3	14.0	79.1	0.09	-

^{*}The ratio of metal to phenol (MTP, mol: mol) expressed in percentages;


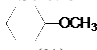
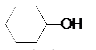
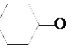
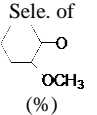
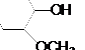
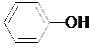
^{**}The catholyte is 0.1 mol l⁻¹ H₃PO₄ without SiW₁₂;

[†]The catholyte is 1 mol l⁻¹ H₃PO₄ without SiW₁₂;

[‡]No suspended Pt/C catalyst;

^{††}The catholyte is 0.1 mol l⁻¹ triflic acid without SiW₁₂;

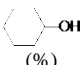
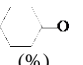
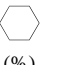
Table S2 Electro-hydrogenation of guaiacol over commercial catalysts under different conditions. The catholyte: 10 ml SiW₁₂ (0.1 mol l⁻¹) solution; anolyte: 1 mol l⁻¹ H₃PO₄.

Entry	Cat., MTG (%) [*]	<i>T</i> (°C)	<i>I</i> (mA cm ⁻²)	<i>P</i> (V vs. NHE)	Reac. Time (min)	Conv. (%)	Sele. of  (%)	Sele. of  (%)	Sele. of  (%)	Sele. of  (%)	Sele. of  (%)	Sele. of  (%)	Sele. of  (%)	F.E. (%)
23 [†]	Pt/C, 3.5	35	13	-0.274	29.5	8.2	~0	6.2	8.3	67	8.5	7.9	2.1	40.1
24	Pt/C, 3.5	35	100	-0.274	25	93.5	17.4	9.0	50.2	8.7	10.5	4.0	0.3	92.1
25	Pt/C, 3.5	35	150	-0.311	15	92.9	10.4	8.6	56.0	6.5	14.0	4.5	0.0	98.6
26	Pt/C, 3.5	35	200	-0.347	12	98.9	6.8	10.3	54.3	9.3	14.1	4.8	0.4	96.3
27	Pt/C, 3.5	35	250	-0.385	16.7	94.9	7.0	8.9	55.1	7.7	15.3	4.5	1.5	55.0
28	Pt/C, 3.5	55	250	-0.373	9.2	94.6	11.6	8.3	56.0	7.6	11.7	4.3	0.5	95.6
29	Pt/Al ₂ O ₃ , 5	55	100	-0.269	25	95.2	7.1	4.2	59.5	17.2	5.9	2.3	3.8	89.3
30	Pd/C, 10	55	100	-0.273	16.7	95.0	0.0	2.2	3.7	48.0	43.7	0.0	2.4	94.4
31	Rh/C, 5	55	100	-0.291	21.7	94.3	10.5	15.5	23.3	4.7	33.8	12.1	0.1	91.2

^{*}The ratio of metal to guaiacol (MTG, mol: mol) expressed in percentages.


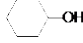
[†]The catholyte is 0.1 mol l⁻¹ H₃PO₄ without SiW₁₂.

Table S3 Electrolytic hydrogenation of phenol over different catalysts in published researches

Entry	Phenol (mmol l ⁻¹)	Cat., MTP (%)	<i>T</i> (°C)	<i>I</i> (mA cm ⁻²)	<i>P</i> (V vs. NHE)	Reac. Time (min)	Conv. (%)	Sele. of  (%)	Sele. of  (%)	Sele. of  (%)	F.E. (%)	Rate (mmol g _M ⁻¹ s ⁻¹)	TOF (h ⁻¹)
Ref (15)*	17.7	Pt/C, 1.2	25	40mA	-0.48	150	~30				40	0.015	28.8
Ref (15)*	17.7	Rh/C, 2.4	25	40mA	-0.45	150	~40				52	0.018	34
Ref (2), Ref (10)*	16	Rh/C, 20mg	25	0.02	-0.2	150	~10				20	0.0081	15
Ref (2), Ref (10)*	16	Rh/C, 20mg	25	0.25	-0.7	60	~100				66	0.34	629
Ref (3)	100	0.5mg cm ⁻²	80	18.9			18	80			30	0.02	34.6
Ref (3)	100	0.5 mg Pd cm ⁻²	80	18.9			28	80			30	0.022	22.2

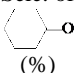
*Reference (10,15) in manuscript.

Table S4 Electro-hydrogenation of cyclohexanol and cyclohexanone over commercial catalysts under different conditions. The catholyte: 10 ml SiW₁₂ (0.1 mol l⁻¹) solution; anolyte: 1 mol l⁻¹ H₃PO₄.

Entry	Substrate	Substrate conc. (mmol l ⁻¹)	Cat., MTC (%) [*]	<i>T</i> (°C)	<i>I</i> (mA cm ⁻²)	<i>P</i> (V vs. NHE)	Reac. Time (min)	Conv. (%)	Sele. of  (%)	Sele. of  (%)	F.E. (%)
32	cyclohexanol	20	Pt/C,5	55	50	-0.178	15	16.8	~100	-	14.4
33	cyclohexanol	20	Pt/C,5	75	50	-0.153	15	25.7	~100	-	21.9
34	cyclohexanol	20	Pt/C,5	95	50	-0.132	15	52.6	~100	-	45.1
35	cyclohexanone	20	Pt/C,5	55	50	-0.179	14	>99	13.5	86.5	>99

^{*}The ratio of metal to cyclohexanol or cyclohexanone (MTC, mol: mol) expressed in percentages.

Table S5 Thermal selective hydrogenation of phenol to cyclohexanone over different catalysts in published researches

Entry	Phenol (mmol l ⁻¹)	Catalyst (mg)	<i>T</i> (°C)	<i>P</i> (V)	Reac. Time (min)	Conv. (%)	Sele. of  (%)	Rate (mmol g _M ⁻¹ s ⁻¹)	TOF (h ⁻¹)
Ref (27)*	500 in water	Pd colloid	90	0.1 Mpa H ₂	960	99.7	99.5	0.0077	7.8
Ref (28)*	250 in water	Pd/silica	35	0.1 Mpa H ₂	300	70	99	0.024	21.8
Ref (29)*	66.7 in water	Pd/HPA**	75	0.1 Mpa H ₂	180	100	100	0.044	13.3
Ref (30)*	1000 in CH ₂ Cl ₂	Pd/C+AlCl ₃	100	0.5 Mpa H ₂	60	99	99.2	0.0524	-
Ref (31)*	250 in water	Pd/C ₃ N ₄	100	0.1 Mpa H ₂	60	99	99	0.0524	123.2

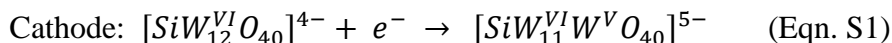
*References in manuscript.

**HPA is Hydroxyapatite. The reaction rates and TOF cited in references are recalculated based on weight and particle size of catalyst metals.

Supporting Text

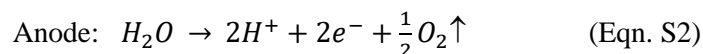
1. Electron and proton transfer between anode and cathode compartment during the electrolysis

To investigate the proton transfer during the electrolysis, pH value was monitored at both anode and cathode sides. The results are shown in Fig. S4. During the time from initial to 40 min, the cathode electrolyte was SiW₁₂ solution without Pt/C catalyst under the electrolysis at 100 mA cm⁻² and protection of ultrapure N₂ atmosphere. The reaction that occurred in cathode at this time is the electric reduction of SiW₁₂, according to the first wave in CV measurement shown in Fig. S3:

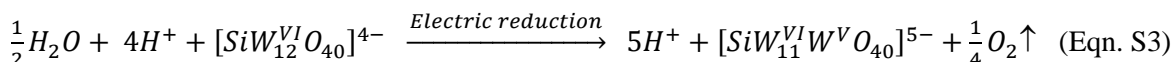


Literature reported that silicotungstic acid (SiW₁₂) is significantly stronger than ordinary mineral acids, and the protons of SiW₁₂ are completely dissociated in aqueous solution^{4,7}. Therefore, the ionic chemical formulas were used to describe the status of SiW₁₂ in aqueous solution.

At anode, the reaction is water electric oxidation:

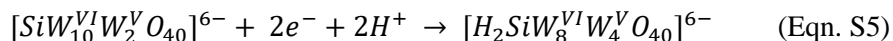
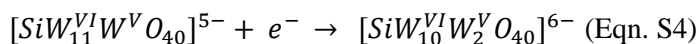


The produced proton diffuses under the electric field from anode to cathode through Nafion membrane, maintaining the charge balance of both sides. Therefore, the cathode solution was changed from initial SiW₁₂ solution to reduced SiW₁₂ solution:

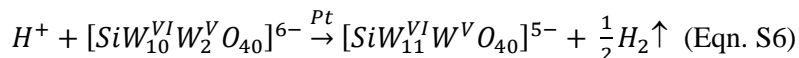


SiW₁₂ and one-electron reduced SiW₁₂ are super strong acids that almost all of the protons are dissociated into water. Therefore, the H⁺ concentration was gradually increased and thus the pH value decreased at the cathode side during electrolytic time. For example, the initial concentration of [SiW₁₂^{VI}O₄₀]⁴⁻ is 0.1 mol l⁻¹ so the H⁺ concentration is 0.4 mol l⁻¹. After electrolytic reduction, the reductive state of [SiW₁₁^{VI}W^VO₄₀]⁵⁻ was formed so the H⁺ concentration is 0.5 mol l⁻¹ at this time. However, the pH value maintains stable at anode because the proton comes from splitting of water not from H₃PO₄.

SiW₁₂ can be further reduced on cathode electrode, corresponding to the second and third waves in CV measurement of SiW₁₂:

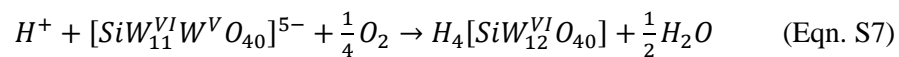


When Pt/C catalyst was added into the reduced SiW₁₂ solution, hydrogen gas evolved out. The reaction can be determined based on reduction degree measurement of SiW₁₂ in our experiment:



The reduced SiW₁₂ can be recycled between the cathode electrode and Pt/C catalyst to continuously produce hydrogen gas. Because the hydrogen evolution reaction over Pt/C is a super-fast reaction that the reaction rate reaches 2.8 mol (hour, mg-Pt)⁻¹, further reduced SiW₁₂ species will not be accumulated and [SiW₁₁^{VI}W^VO₄₀]⁵⁻ will be the main reduced form of SiW₁₂ in the solution. Therefore, when the electrolysis of SiW₁₂ solution with Pt/C, pH value maintains stable, as shown in Fig S4.

After the electrolysis, if the solution was exposure to air, oxidation reaction accompanying with the proton consuming occurs according to the overall oxidation reaction equation:



This is the reason that pH value raises shown in Fig. S4.

2. Chemical analysis of products using Gas chromatography (GC)

Gas chromatography (GC) was used to quantitatively analyze products in the phenol electrolysis. The average response factors were measured with internal standard (n-decane) by repeating 3 times. The values were calculated according to Eqn. S8, showing the average factors are 1.00, 1.07, 1.07, 1.08 for phenol, cyclohexanol, cyclohexanone and cyclohexane respectively. The response factors can be recognized as 1 in the study. Therefore, the normalization method (without internal standard) can be used for quantitative analysis of conversion and selectivity.

$$f_m = \frac{A_s \times m_i}{A_i \times m_s} \quad (\text{Eqn. S8})$$

Where A_i and m_i are GC peak area and mass of target component respectively;
 A_s and m_s are GC peak area and mass of internal standard respectively.

To calculate conversion and selectivity of other unsaturated compounds hydrogenation, the effect carbon number method (ECN) (S8) with internal standard (n-decane) was used, because of lack of standard chemicals for all generated products to measure the response factor. The Equations S9-S11 are used in the calculation.

$$n_i = \frac{A_i}{A_D} \times \frac{W_D}{MW_D} \times \frac{ECN_D}{ECN_i} \quad (\text{Eqn. S9})$$

$$\text{Conversion} = \left(1 - \frac{n_0}{n_{ini}}\right) \times 100\% = \left(1 - \frac{f \times A_0 \times m_s}{A_s \times m_{ini}}\right) \times 100\% \quad (\text{Eqn. S10})$$

$$\text{Selectivity} = \frac{\frac{A_i}{ECN_i}}{\sum \frac{A_i}{ECN_i}} \times 100\% \quad (i = 1, 2, 3 \dots) \quad (\text{Eqn. S11})$$

Where n_0 is the mole number of the substrate detected in analyzed samples; n_i is the mole number of produced products in analyzed sample; n_{ini} and m_{ini} is the initial added mole number and mass of the substrate respectively;

A_0 is the peak area of the substrate detected in analyzed samples; A_i is the peak area of produced products in analyzed sample measured by GC-FID chromatogram;

ECN_i are effective carbon numbers of produced products;

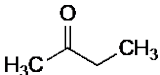
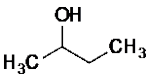
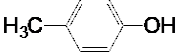
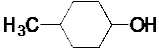
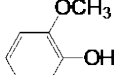
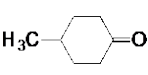
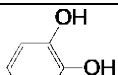
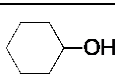
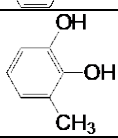
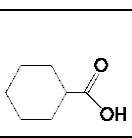
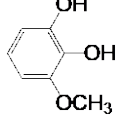
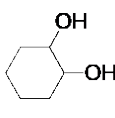
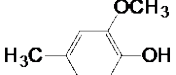
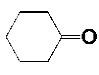
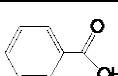
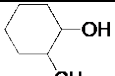
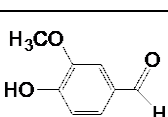
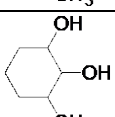
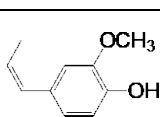
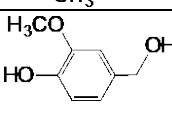
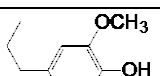
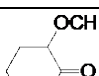
A_D , W_D , MW_D and ECN_D are the peak area, mass, molecular weight and effective carbon number of n-decane.

The calculation of ECN is based on group contributions, as shown in Table S6. Table S7 shows some examples of calculated ECNs values that used in this study.

Table S6 Contributions to the effective carbon number (ECN)

Atom-in-groups	ECN contribution	Atom-in-groups	ECN contribution
Carbon-Aliphatic	1	Oxygen-primary alcohol	-0.5
Carbon-Aromatic	1	Oxygen-phenol	-1
Carbon-Olefinic	0.95	Oxygen-ether	-1
Carbon-Carbonyl	0	Carbon-Carboxyl	0
Oxygen-Secondary alcohol	-0.75	Oxygen-Tertiary alcohol	-0.25

Table S7 Examples of effective carbon number used in GC analysis

Compounds	Calculated ECN	Compounds	Calculated ECN
	3		3.25
	6		6.25
	5		6
	4		5.25
	5		6
	4		4.5
	6		5
	6		6.25
	5		5
	7.9		5.5
	8		5

3. Studies of Phenol consuming in the electrolysis

The phenol concentration was monitored during the electro-hydrogenation. The results (Fig. S16) show the phenol concentration drops linearly versus time in the reaction, which indicates the phenol electro-hydrogenation is a zero-order reaction. The apparent hydrogenation rate (r) can be expressed as:

$$r = -\frac{d[\text{phenol}]}{d[t]} = k \quad (\text{Eqn. S12})$$

where k is a constant. Integrating both sides of the equation S12, we can obtain:

$$[\text{phenol}]_t = -kt + [\text{phenol}]_0 \quad (\text{Eqn. S13})$$

where $[\text{phenol}]_t$ is the phenol concentration at the reaction time t ; $[\text{phenol}]_0$ is initial phenol concentration.

The apparent phenol hydrogenation rate can be calculated by linear fitting the phenol concentrations. The zero-order reaction rate in kinetics suggests the phenol hydrogenation reaction is highly dependent of the catalyst which limits the number of reactant molecules that can react at a time. Therefore, the specific reaction rate was calculated on a basis that is not the volume of the reactor but on the catalyst weight ($\text{mol g}^{-1} \text{s}^{-1}$):

$$\text{reaction rate} = \frac{\text{consumed substrate (mol)}}{\text{reaction time (s)} \times \text{mass of catalytic metal(g)}} \quad (\text{Eqn. S14})$$

This equation is equal to equation 3 in the manuscript which was used in the reaction rate calculation.

Different reaction rates under various electric current densities were calculated (Fig. S16). The reaction rate almost linearly increases with the increasing of electric current density. However, the reaction rate reaches the highest value at 180 mA cm^{-2} , and then the reaction rate decreases with the increasing of current density up to 250 mA cm^{-2} . The reaction rate decrease is possibly caused by the production of hydrogen bubble on the catalyst surface which hinder the diffusion of phenol and products.

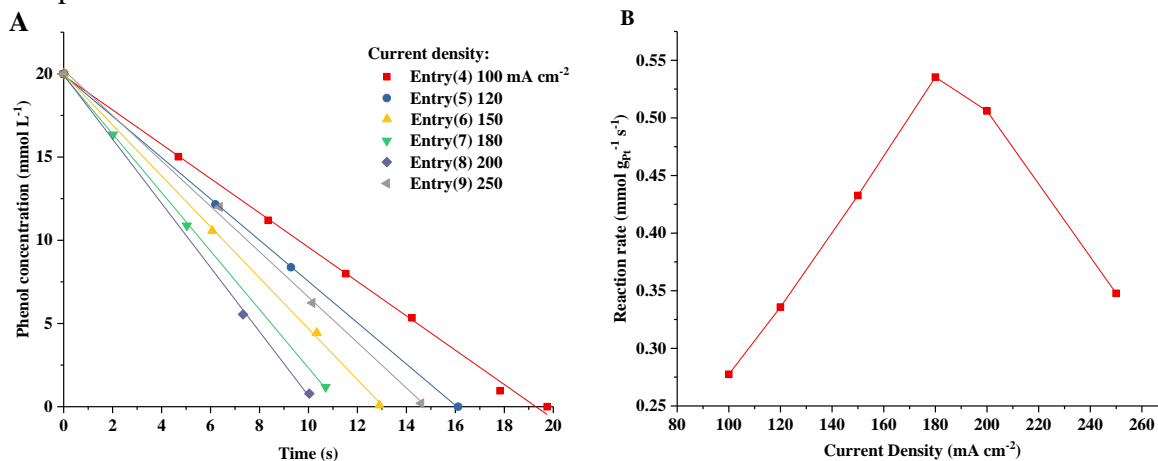


Figure S16 Phenol concentration drop during the electro-hydrogenation process with different current density (at 35°C) (A) and different reaction rates under various electric current densities (B). The detail reaction conditions are shown in Table S1 entry 4-9.

4. Turnover rates investigation

Turnover frequency (TOF) is the rate referred to the number of catalytic sites, which is defined as the number of molecules of a specified product made per catalytic site and per unit time⁸. It can be expressed as:

$$TOF = \frac{[\#reacted\ molecules]}{[\#active\ sites] \times [\#unit\ time]} \quad (\text{Eqn. S15})$$

The difficulty in TOF measurement is not only in determining the reaction rate but also in counting active sites. The active sites can be approximately recognized as the number of metal atoms (Pt, Pd or Rh in this study) on the catalyst surface. Therefore, the number of active sites can be calculated:

$$[\# \text{ active sites}] = D \times [\# \text{ metal atoms}] \quad (\text{Eqn. S16})$$

where D is the degree of dispersion which is the percentage of exposed atoms of supported metal catalyst.

Substituting equation (S16) into (S15), we can obtain:

$$TOF = \frac{\text{Moles of phenol consumed (mol)}}{\text{Time (s)} \times D \times \text{Moles of active metal in the catalyst (mol)}} \quad (\text{Eqn. S17})$$

Equation (S17) is the same as equation (4) in the manuscript that we used in TOF calculation.

The value of D is related to the volume-area mean diameter \bar{d}_{VA} (nm) as following in the spherical metal particle equivalent approximation:

$$D = \frac{6V_M}{A_M} / \bar{d}_{VA} \quad (\text{Eqn. S18})$$

where V_M and A_M are the effective average volume occupied by a metal atom in the surface, and the volume per metal atom in the bulk respectively. The values of $6(V_M/A_M)$ were calculated 1.135 nm for Pt, 1.136 nm for Pd, and 1.098 for Rh⁹

\bar{d}_{VA} can be determined by transmission electron microscopy (TEM, as shown in Fig. S17):

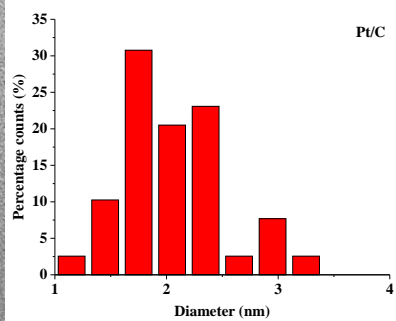
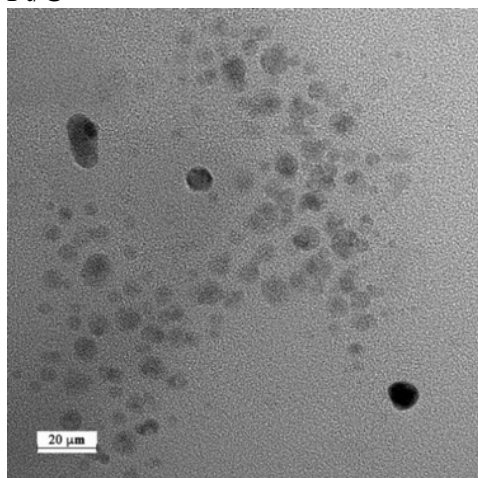
$$\bar{d}_{VA} = \frac{\sum n_i d_i^3}{\sum n_i d_i^2} \quad (\text{Eqn. S19})$$

The calculated \bar{d}_{VA} and degree of dispersion D for different metal catalysts used in this study were summarized in Table S8.

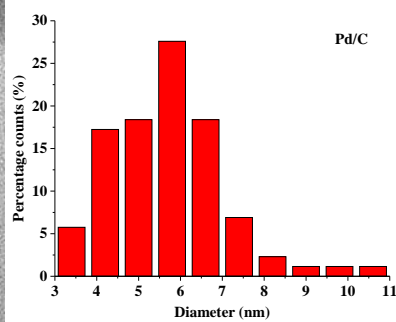
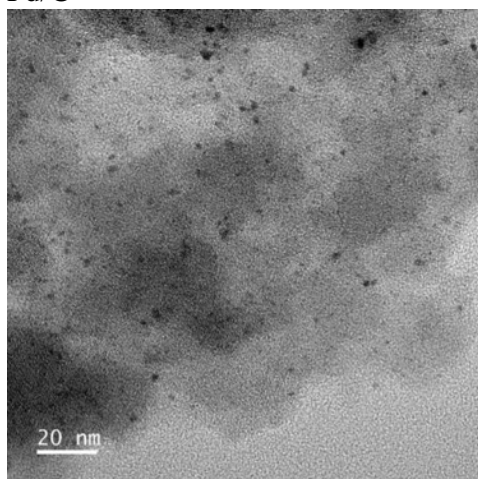
Table S8 Calculated \bar{d}_{VA} and degree of dispersion D for Pt/C, Pd/C and Rh/C catalyst

Catalyst Metal	\bar{d}_{VA} (nm)	D
Pt	2.49	0.4567
Pd	6.95	0.1635
Rh	3.16	0.3478

Pt/C



Pd/C



Rh/C

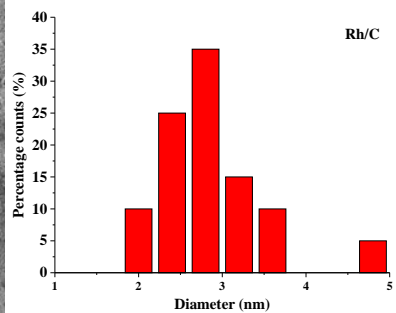
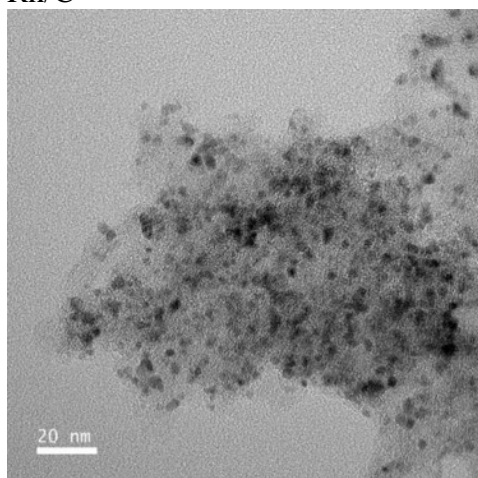


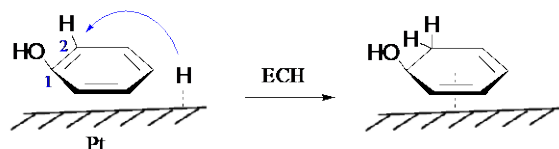
Figure S17 TEM images and metal particle distribution of Pt/C, Pd/C and Rh/C.

5. DFT calculation of electro-hydrogenation-and-hydrodeoxygenation routes

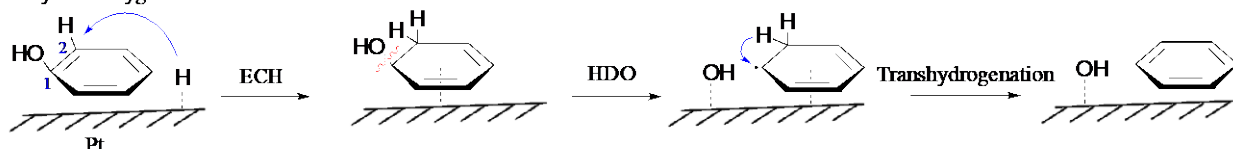
a. Phenol hydrogenation and hydrodeoxygenation

Three pathways were proposed in the phenol hydrogenation and hydrodeoxygenation:

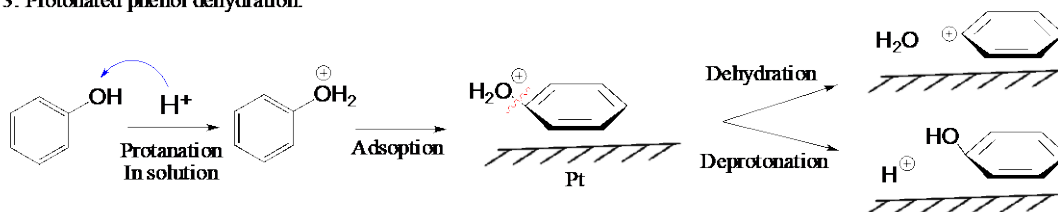
1. Phenol hydrogenation:



2. Hydrodeoxygenation



3. Protonated phenol dehydration:



1. The first pathway shows the first step of phenol hydrogenation. One of the hydrogen atoms was added to the C₂ atom of the phenol molecule. The C atoms were labeled clockwise with consecutive numbers of 1–6, starting with the α -C atom. Theoretically, the hydrogenation could be started at any of the C atom in the phenol molecule. Reported DFT calculations on phenol hydrogenation indicate that C₂ is the most possible started position because this step requires the lowest reaction energy (Ref 31 and 32 in manuscript). The reported results calculated under the condition of gas-phase reactions. Our DFT calculation is on the basis of reported gas-phase results and applied a solvation model to simulate the aqueous environment. The following DFT results are all based on the solvation simulations.

2. The second pathway shows the hydrodeoxygenation of phenol. Previously reported DFT studies suggest the partial hydrogenation and then deoxygenation is the most possible way (Ref 31 and 32 in the manuscript), and the final hydrodeoxygenation product is benzene. Our calculation used the implicit solvation model to evaluate the reaction energy of hydrodeoxygenation in aqueous solution.

3. The third pathway shows the protonation of phenol in aqueous solution. The protonation is possible because the superacid (SiW₁₂) was used in our reaction system. After the protonation, there are two possible reactions: one is the dehydration to form a phenyl cation and the other is deprotonation giving back to a proton and phenol molecule.

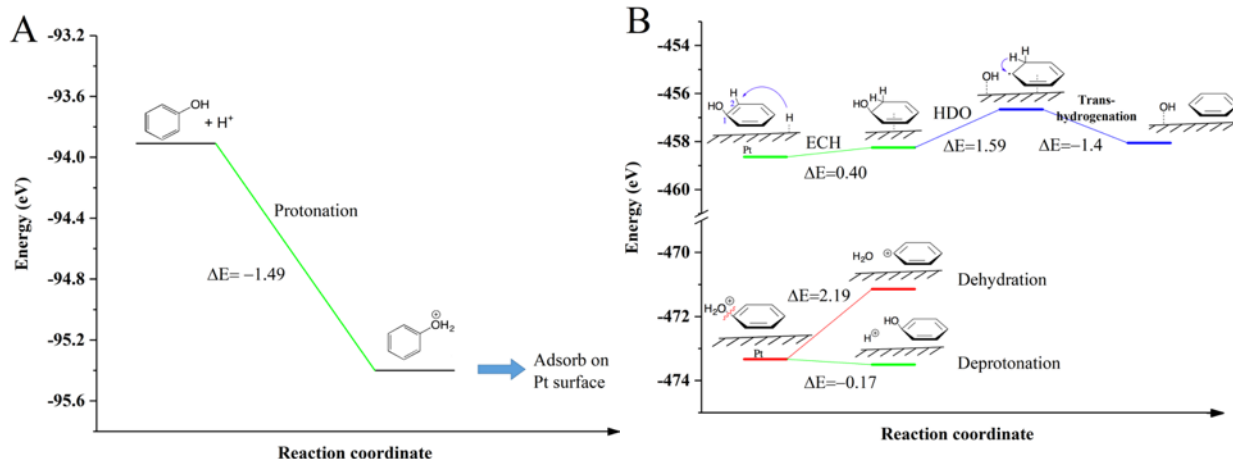


Figure S18 The calculated reaction energy of proposed reaction pathways of phenol. The green line stands for the most possible route in our calculation. The blue line stands for pathway 2, and the red line stands for the phenyl cation formation in pathway 3.

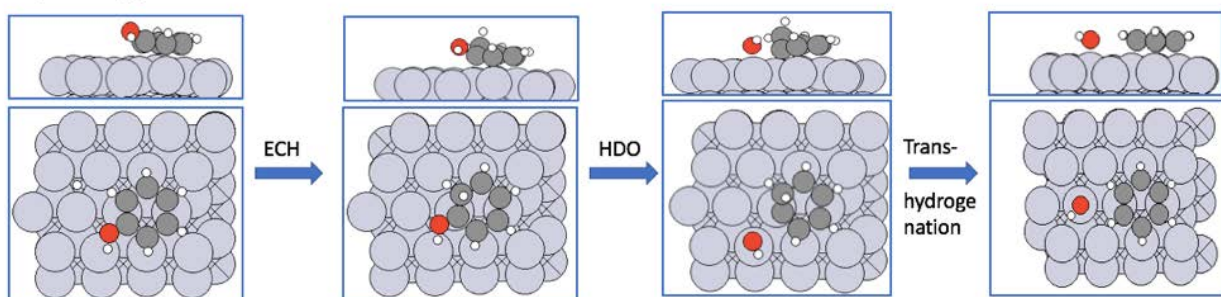
The calculated reaction energies for phenol hydrogenation and deoxygenation are shown in Fig. S18 and the most stable molecular configurations used in the calculation are shown in Fig. S19.

The results suggest:

- (1) The phenol molecule is easy to be protonated in aqueous solution because the reaction energy is -1.49 eV (Fig. S18 (A)). However, after the protonated phenol molecule adsorbed on the Pt(111) surface, it is favorable to be deprotonated (reaction energy -0.17 eV, Fig. S18 (B)). These results suggest the hydrogenation or hydrodeoxygenation of phenol in solution is not in the protonated form. Therefore, the calculations of pathway (1) and (2) were still based on the phenol molecule, not the protonated form.
- (2) The reaction energy of the first step for phenol hydrogenation is 0.40 eV in solution, but the following HDO has a high reaction energy, 1.59 eV. The reaction energy of hydration of protonated phenol to form a phenyl cation shows an expected high value, 2.19 eV. These results indicate that the phenol is possibly hydrogenated to cyclohexanol but not deoxygenation under the calculation conditions.

1. Phenol hydrogenation
The same with the first step in 2. hydrodeoxygenation

2. hydrodeoxygenation



3. Protonated phenol hydration

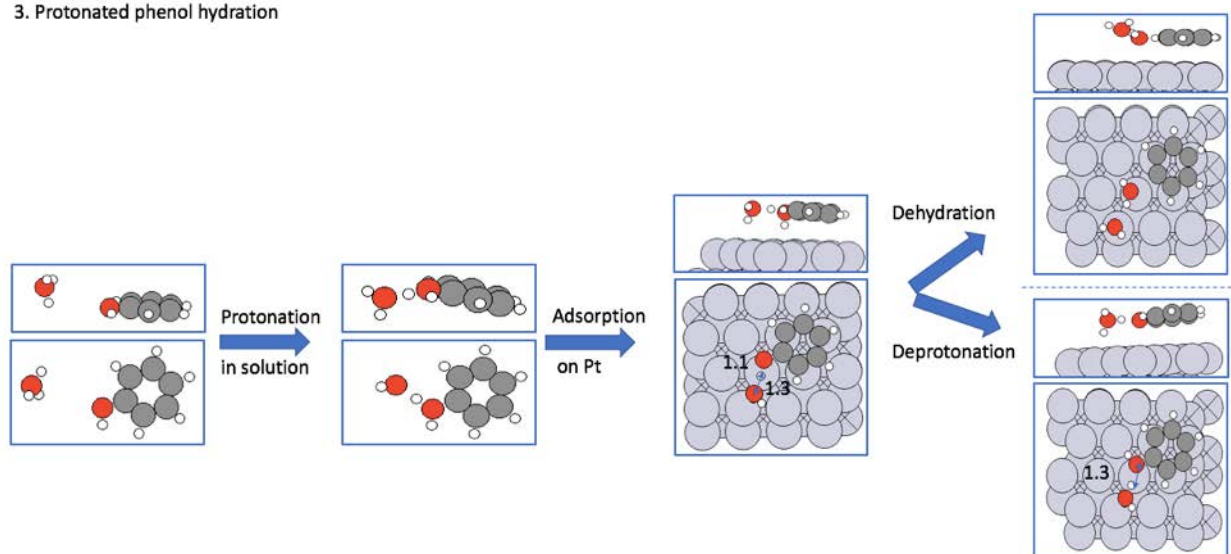
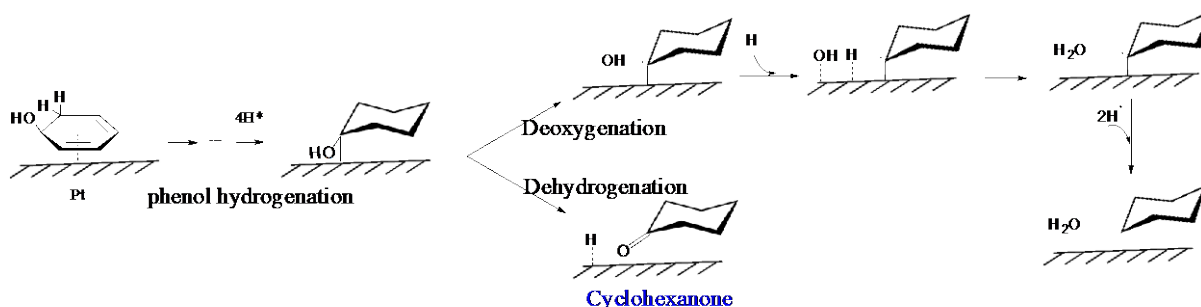


Figure S19 Most stable configuration in the solvated DFT calculation for phenol hydrogenation and hydrodeoxygenation. The Pt, O, H, and C atoms are in lavender, red, white, and gray, respectively, and the unit of distance is Å.

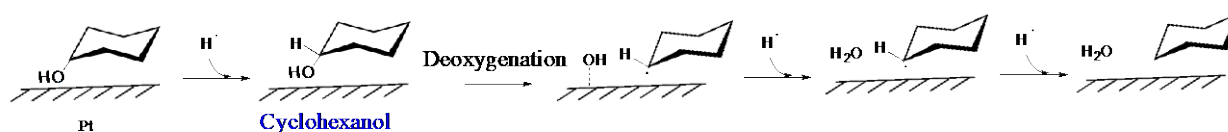
b. Hydrodeoxygenation of cyclohexanol

Three pathways were proposed in the hydrodeoxygenation of cyclohexanol:

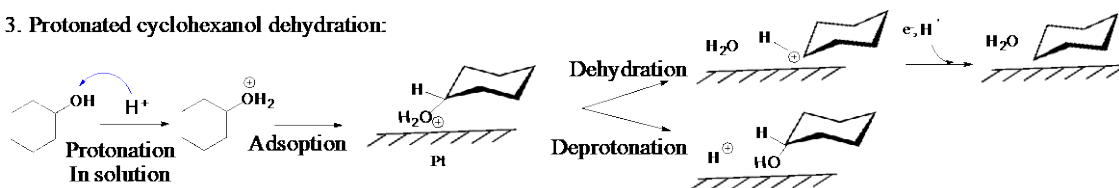
1. Formation of cyclohexanone and deoxygenation



2. Formation of cyclohexanol and deoxygenation



3. Protonated cyclohexanol dehydration:



(1) Because the direct deoxygenation of phenol is energy unfavorable ($E_r = 1.59$ eV), the phenol would be hydrogenated firstly. The benzene ring of phenol can receive five hydrogen atoms, excepting the α -C which is bonded on the Pt surface. At this time, it has two reaction directions: (a) deoxygenation (or de-hydroxylation) and following hydrogenation to yield cyclohexane; (b) dehydrogenation to yield cyclohexanone.

(2) The second reaction pathway includes complete hydrogenation of benzene ring to yield cyclohexanol, and the direct deoxygenation (DDO) of cyclohexanol over Pt surface. This mechanism involves a direct C-O cleavage and then hydrogenation to produce cyclohexane and water.

(3) The third pathway shows the deoxygenation mechanism of protonated cyclohexanol over Pt surface. It is well accepted that the alcohols will be protonated in acidic solution. Therefore, the dehydration of protonated cyclohexanol to give a cyclohexyl cation is possible.

The calculated reaction energies are shown in Fig. S20 and Fig. 5 in the manuscript. The most stable molecular configurations used in the calculation are shown in Fig. S21.

The DFT calculation results suggest:

(1) The deoxygenation in pathway 1 and 2 requires high reaction energy for C-O bond cleavage (0.79 and 0.96 eV respectively).

(2) The reaction energy for C-O bond cleavage through cyclohexyl cation route in protonated cyclohexanol dehydration (pathway 3) is 0.23 eV, which is obviously lower than the value of C-O cleavage in pathway 1 and 2. This indicates that pathway 3 is more favorable than pathway 1 and 2 in the deoxygenation of cyclohexanol.

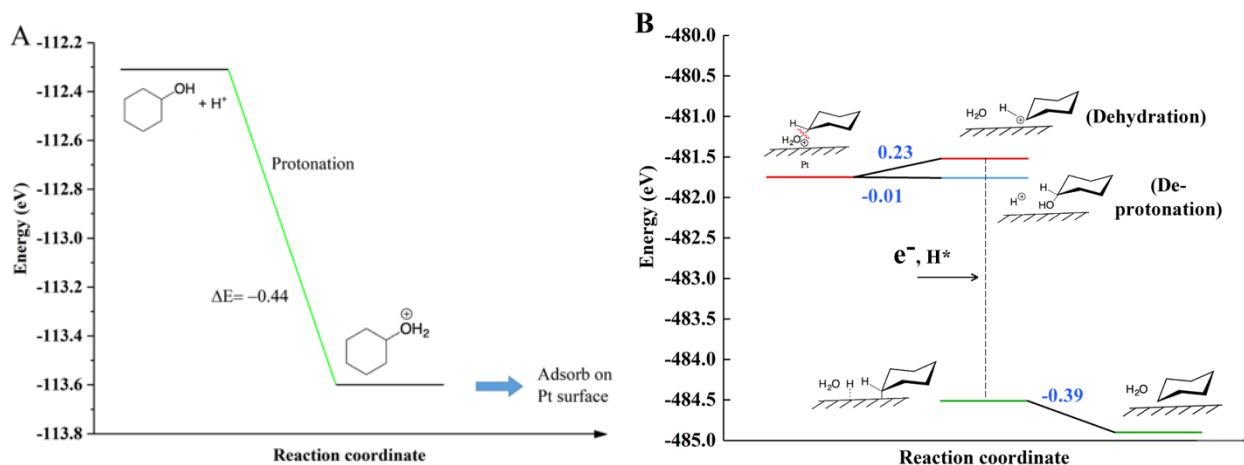
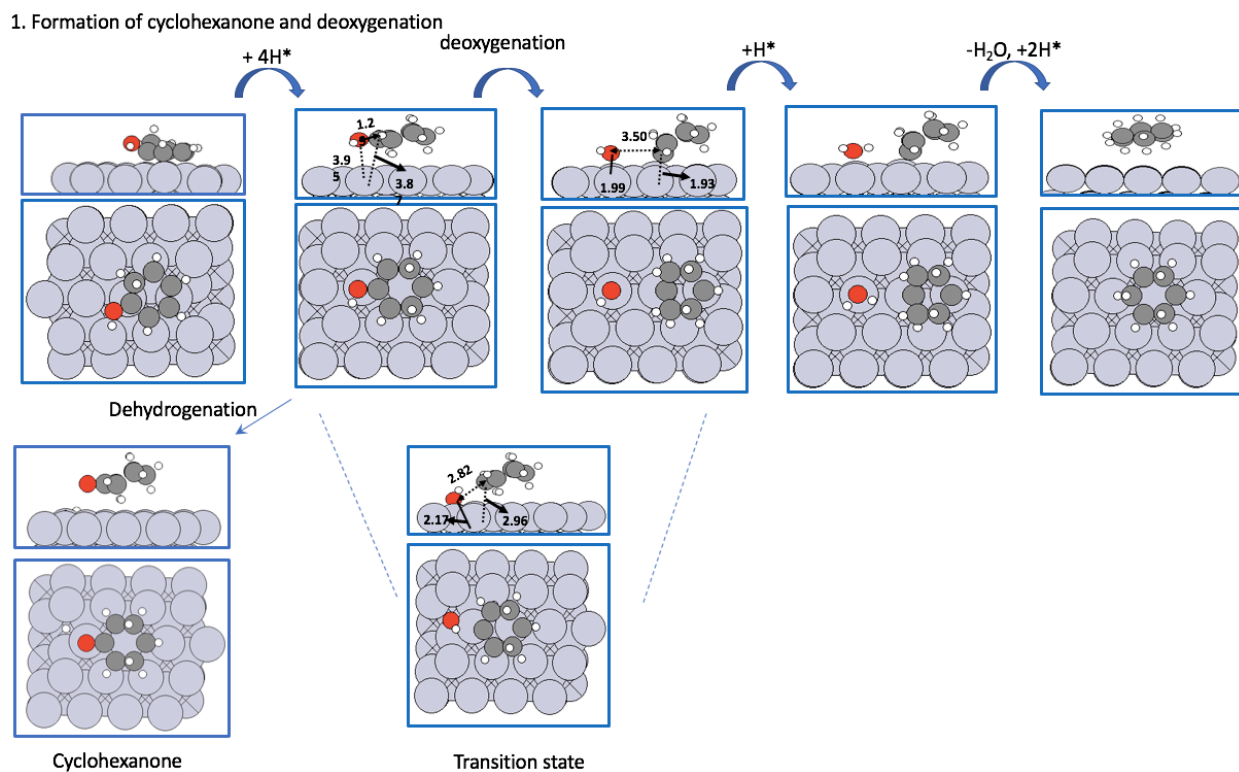
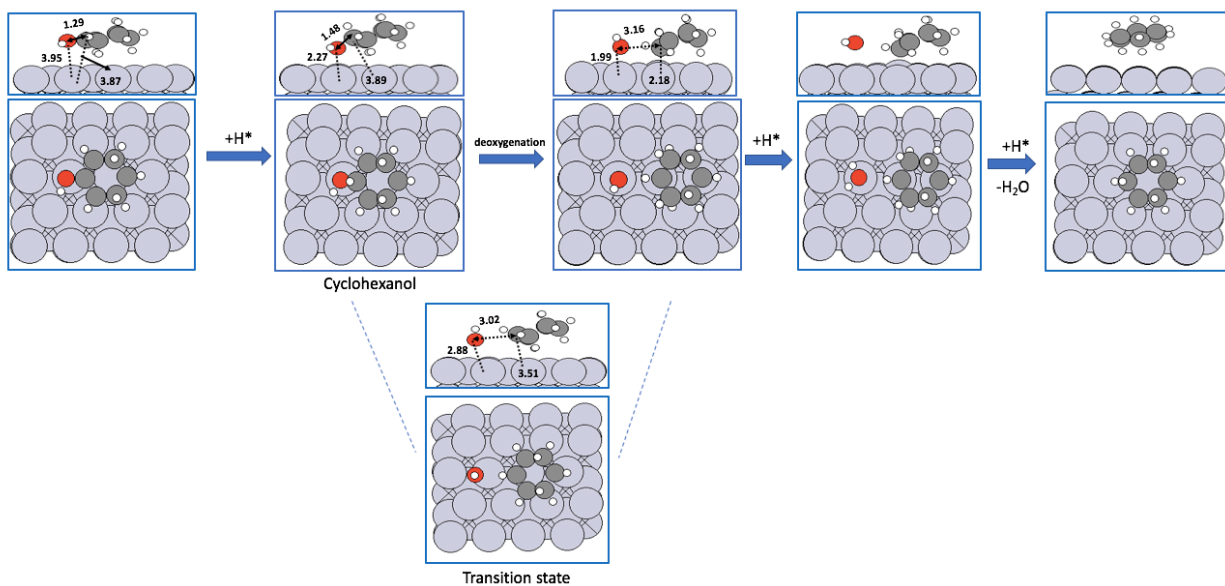


Figure S20 The calculated reaction energy of proposed reaction pathways of cyclohexanol. The results of proposed pathways 1, 2 and 3 are shown as blue, red and green color. The green line shows the most possible deoxygenation route according to the calculated reaction energy.



2. Formation of cyclohexanol and deoxygenation



3. Protonated cyclohexanol dehydration

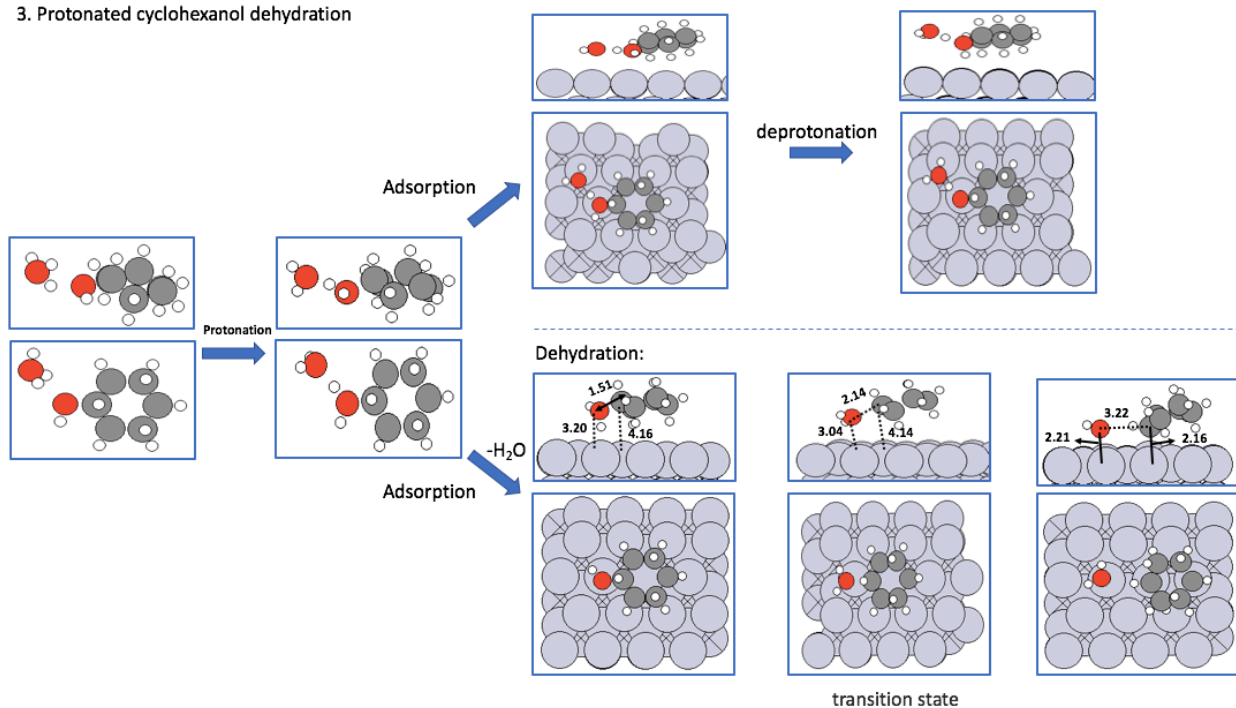
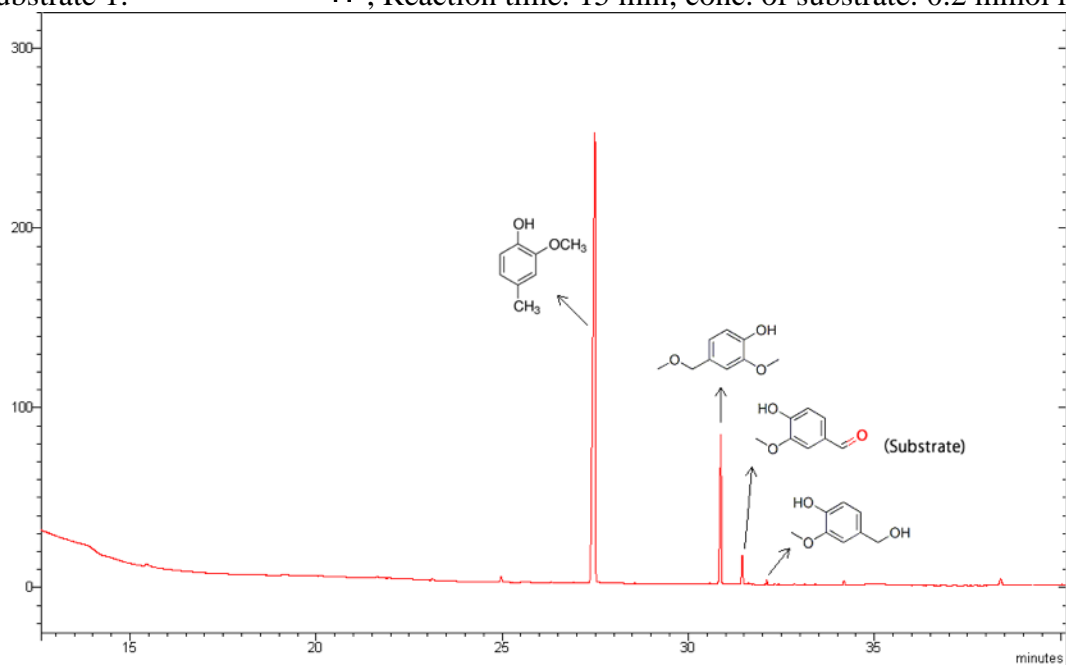
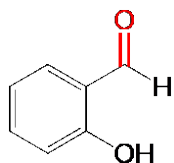


Figure S21 Most stable configuration in the solvated DFT calculation for cyclohexanol hydrogenation and hydrodeoxygenation. The Pt, O, H, and C atoms are in lavender, red, white, and gray, respectively, and the unit of distance is Å.

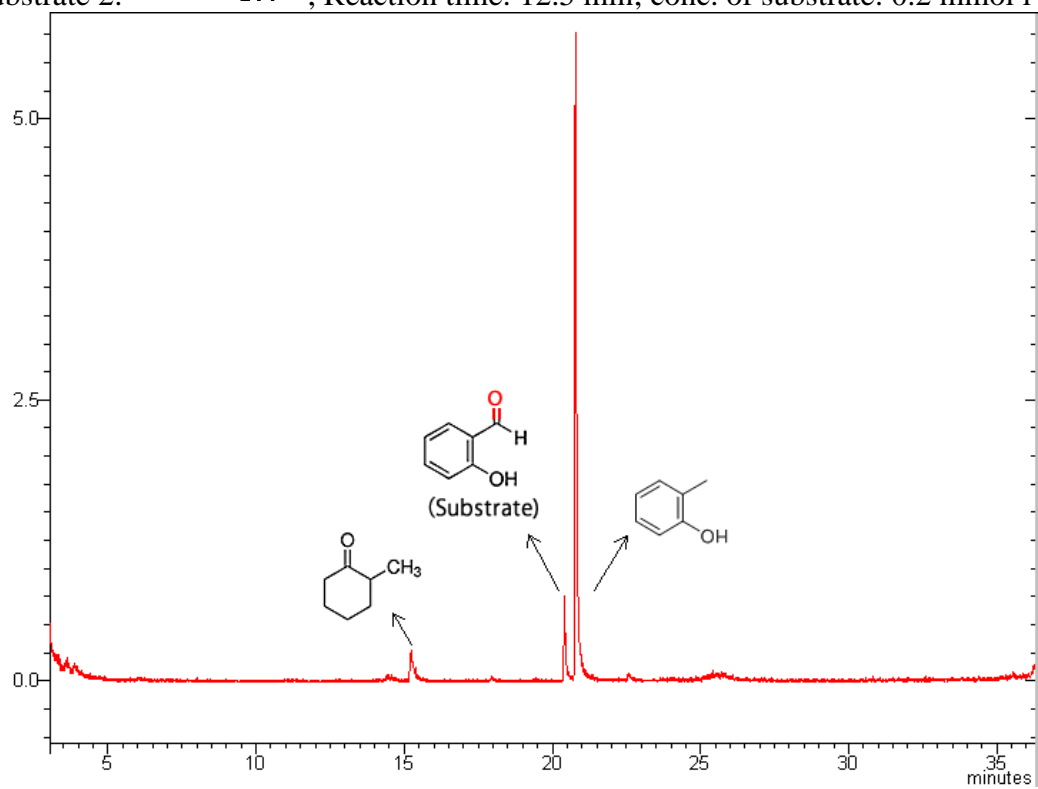
Appendix: GC-MS results for organic substrates electrolysis

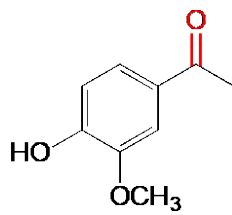
Substrate 1: COc1cc(O)ccc1C=O ; Reaction time: 15 min; conc. of substrate: 0.2 mmol l^{-1}



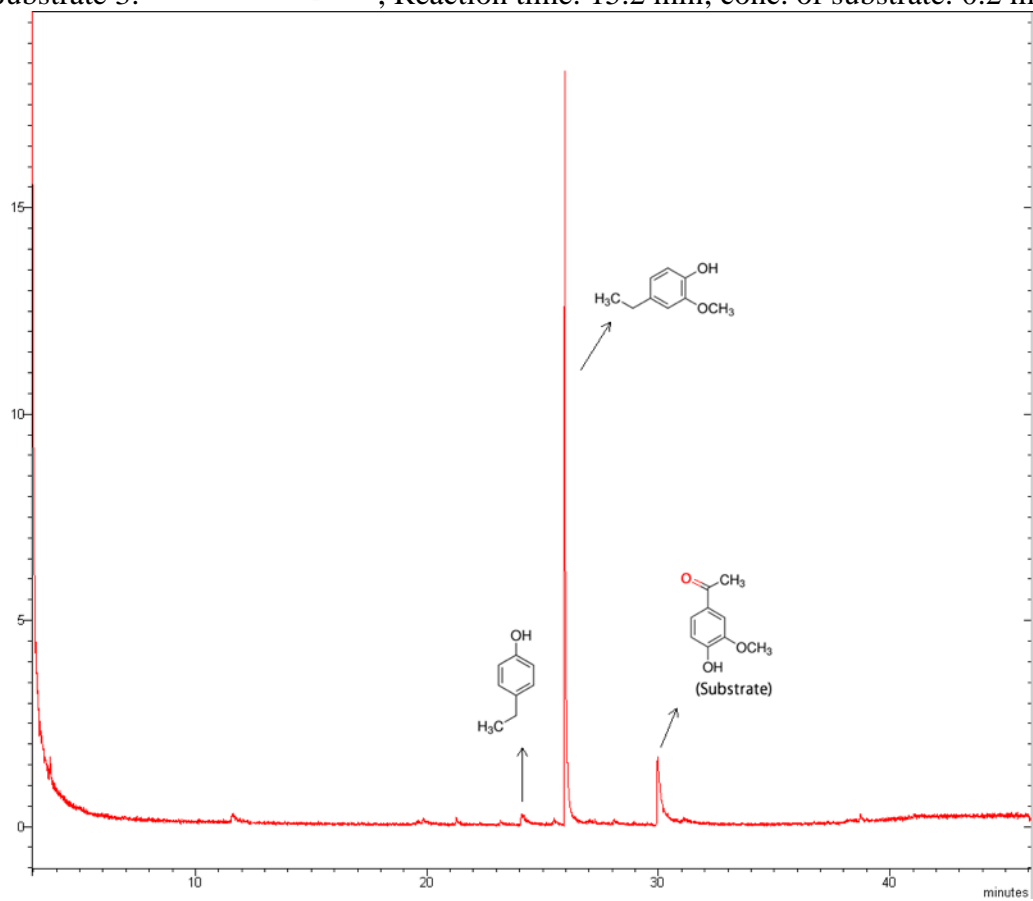


Substrate 2: ; Reaction time: 12.5 min; conc. of substrate: 0.2 mmol l⁻¹

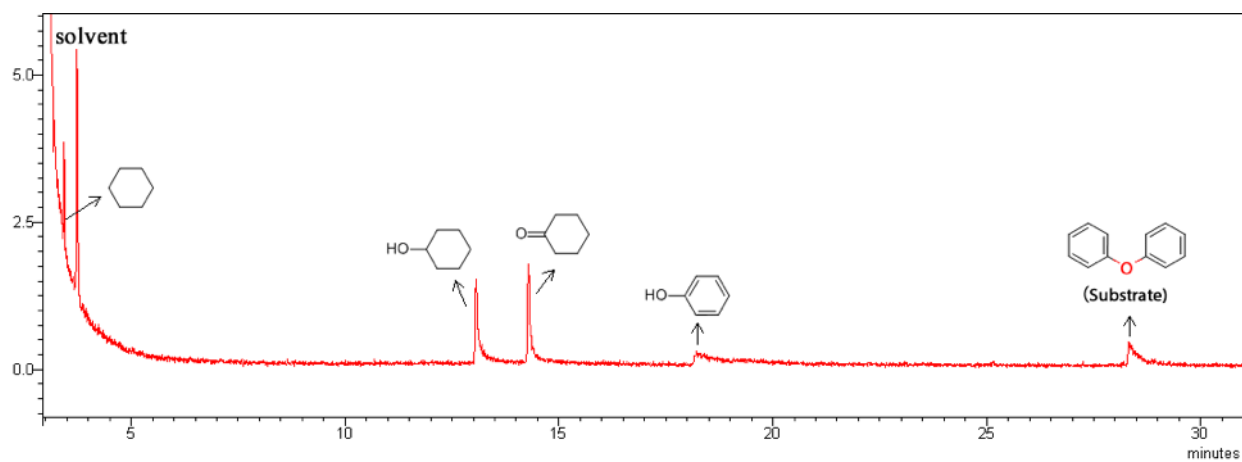




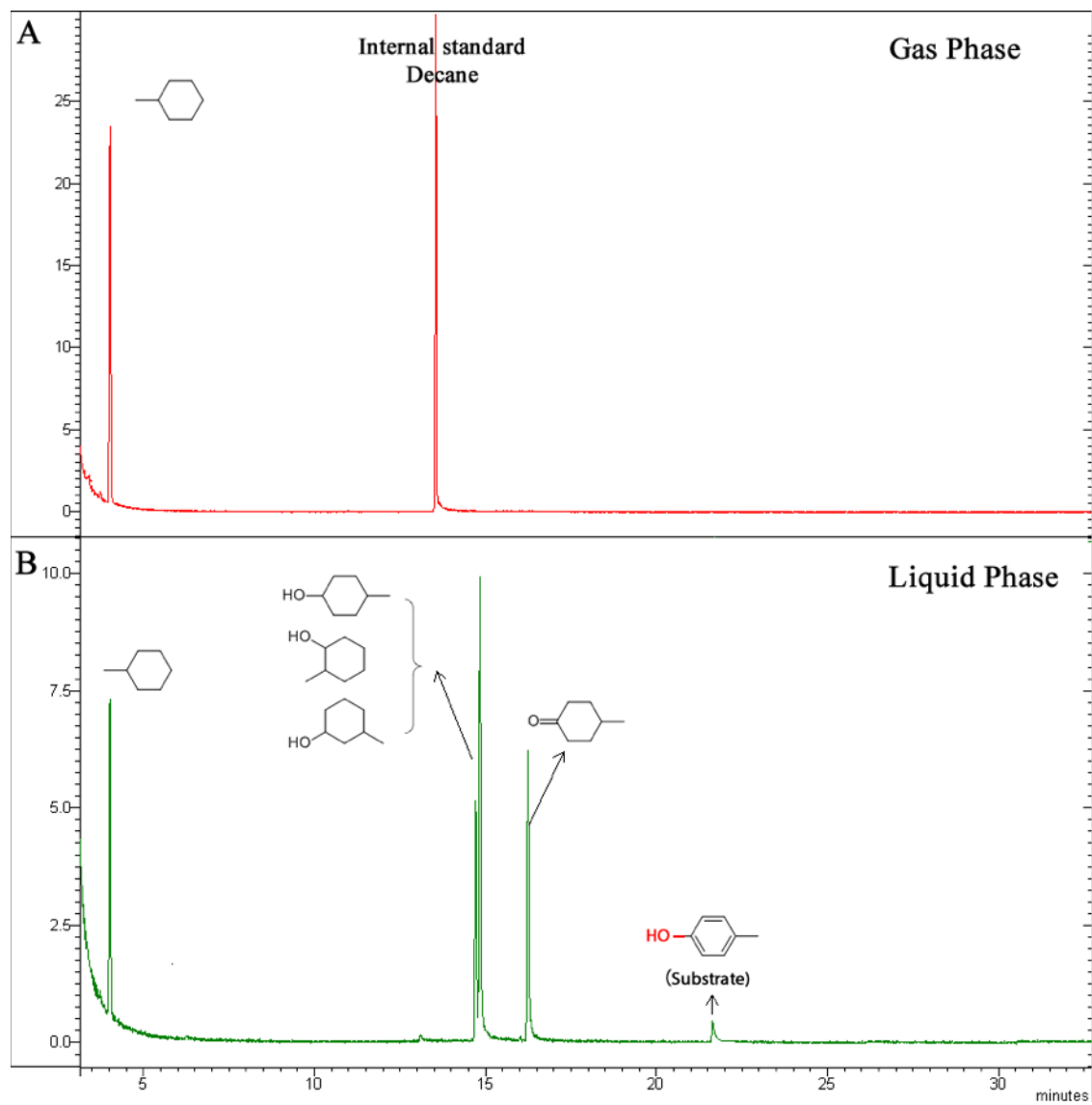
Substrate 3: ; Reaction time: 15.2 min; conc. of substrate: 0.2 mmol l⁻¹



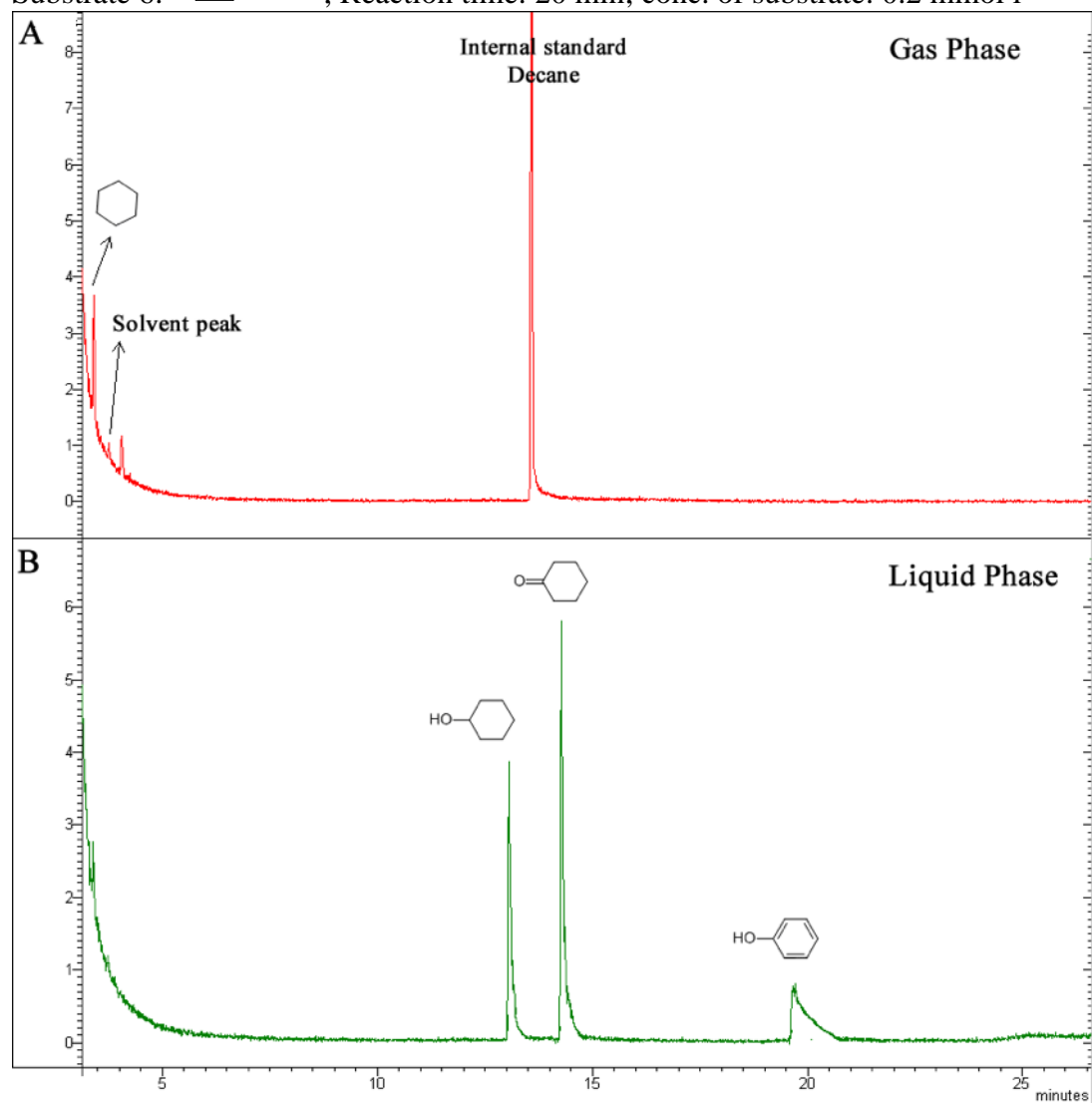
Substrate 4: c1ccc(Oc2ccccc2)cc1; Reaction time: 40 min; conc. of substrate: 0.2 mmol l⁻¹



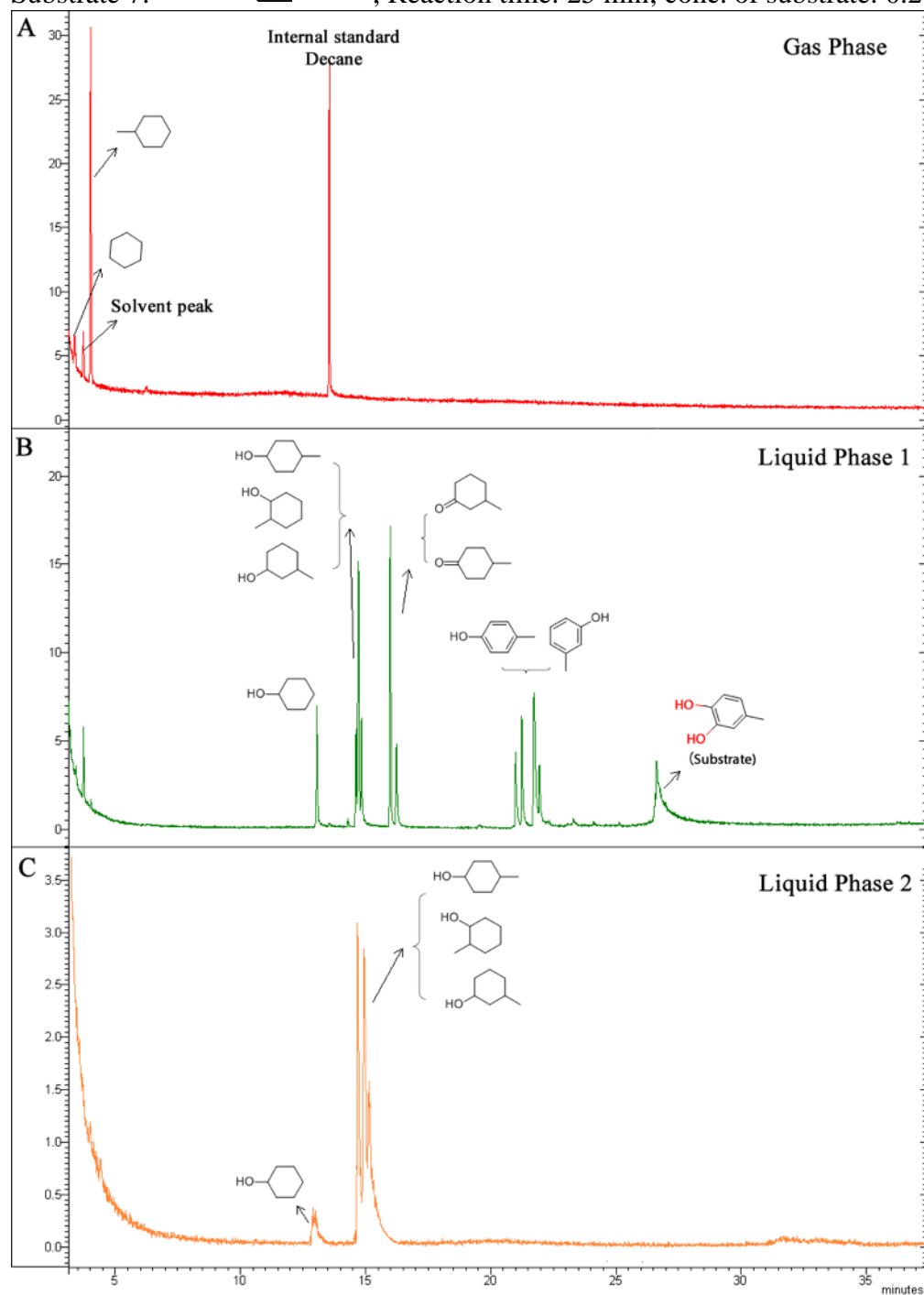
Substrate 5: Cc1ccc(O)cc1; Reaction time: 19.2 min; conc. of substrate: 0.2 mmol l⁻¹

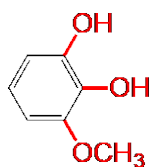


Substrate 6: Oc1ccc(O)cc1; Reaction time: 20 min; conc. of substrate: 0.2 mmol l⁻¹

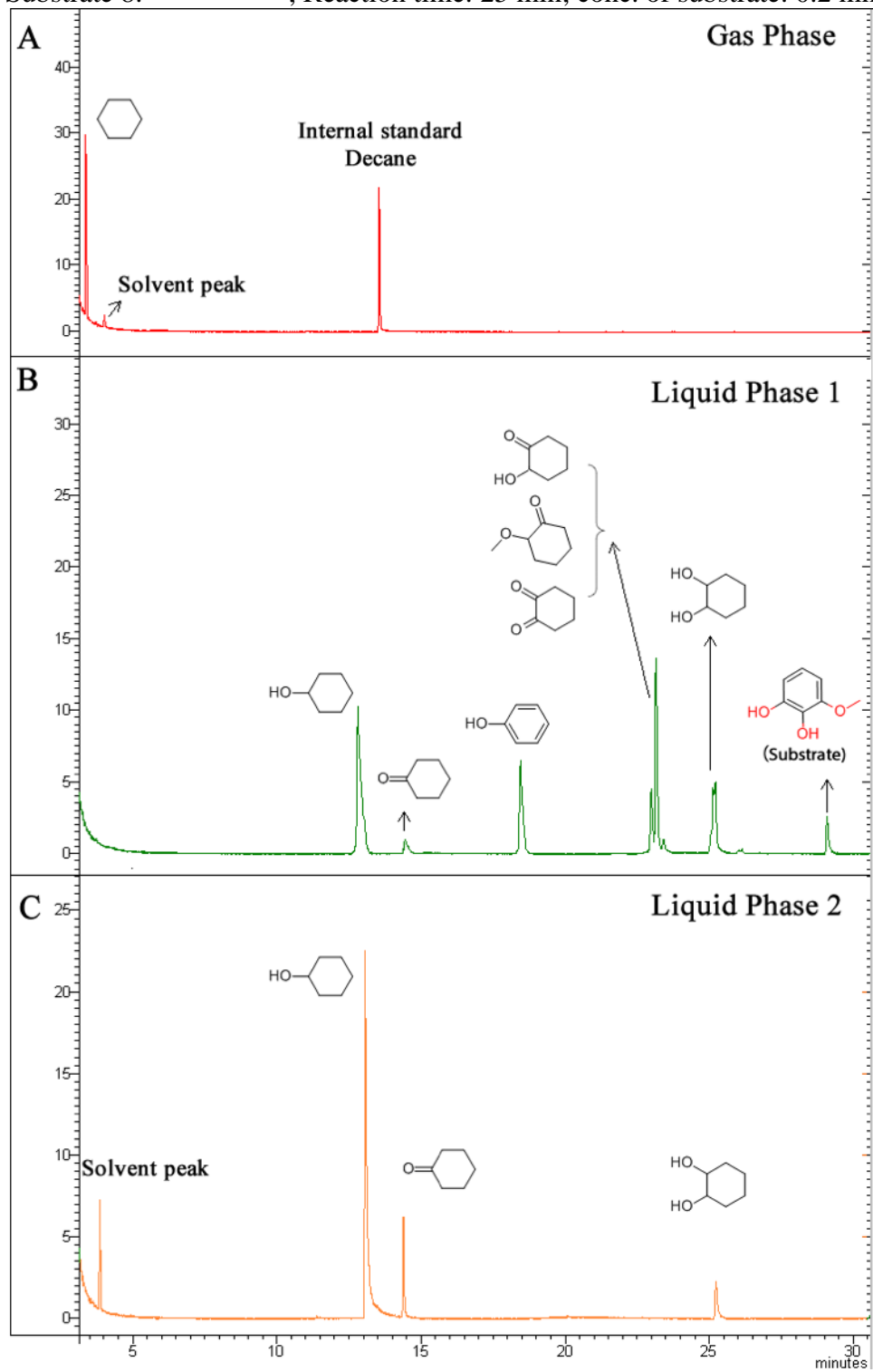


Substrate 7: Cc1ccc(O)c(O)c1; Reaction time: 25 min; conc. of substrate: 0.2 mmol l⁻¹

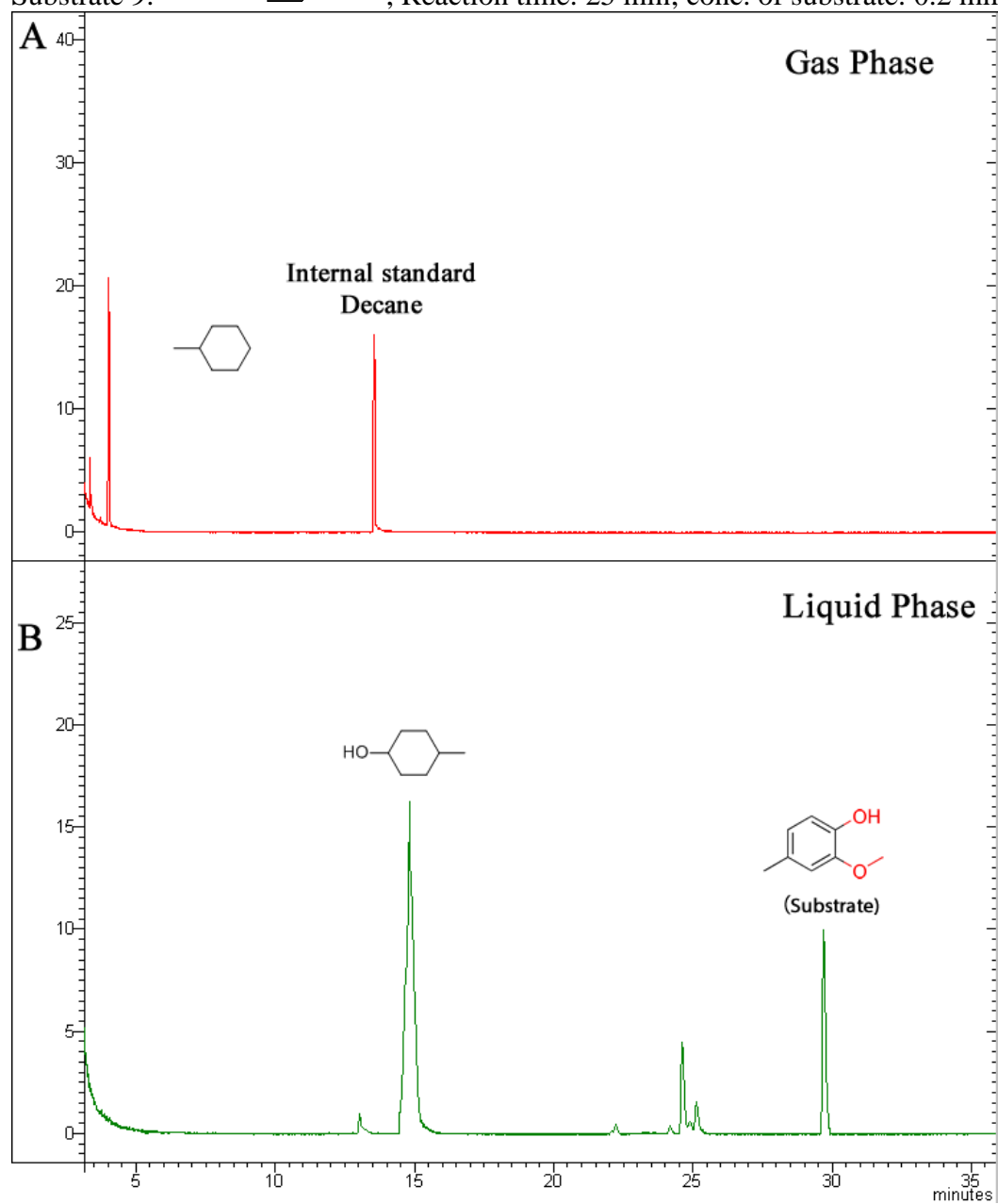




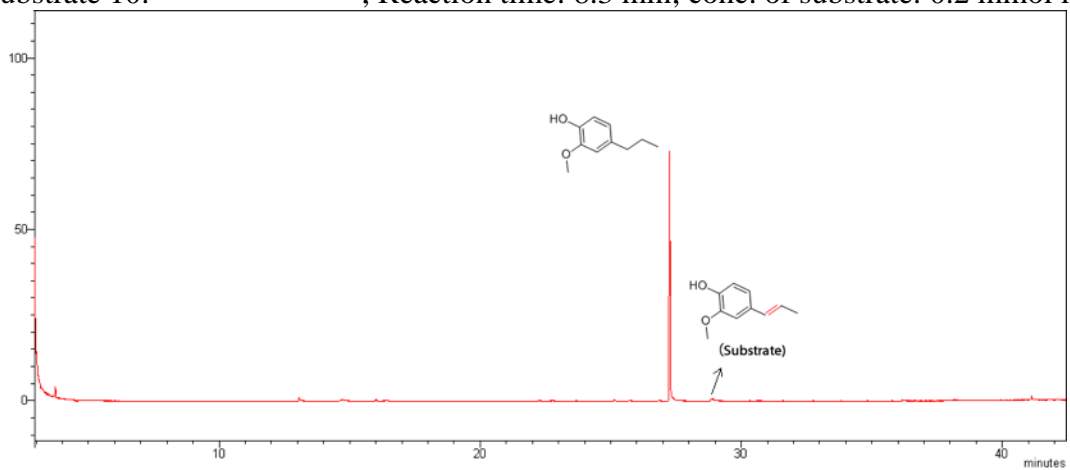
Substrate 8: ; Reaction time: 25 min; conc. of substrate: 0.2 mmol l^{-1}



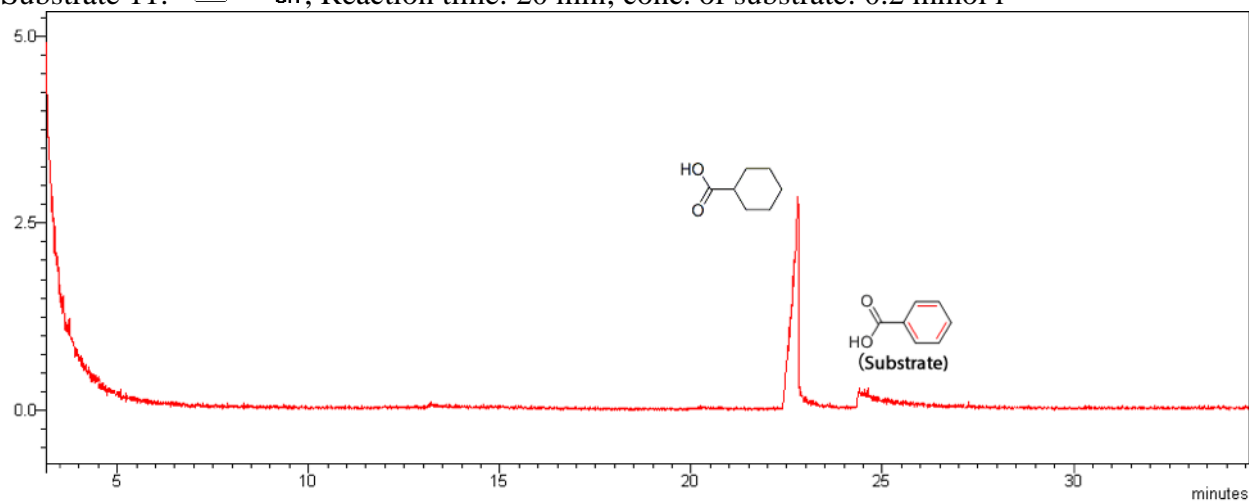
Substrate 9: Cc1ccc(O)c(OC)c1; Reaction time: 25 min; conc. of substrate: 0.2 mmol l⁻¹



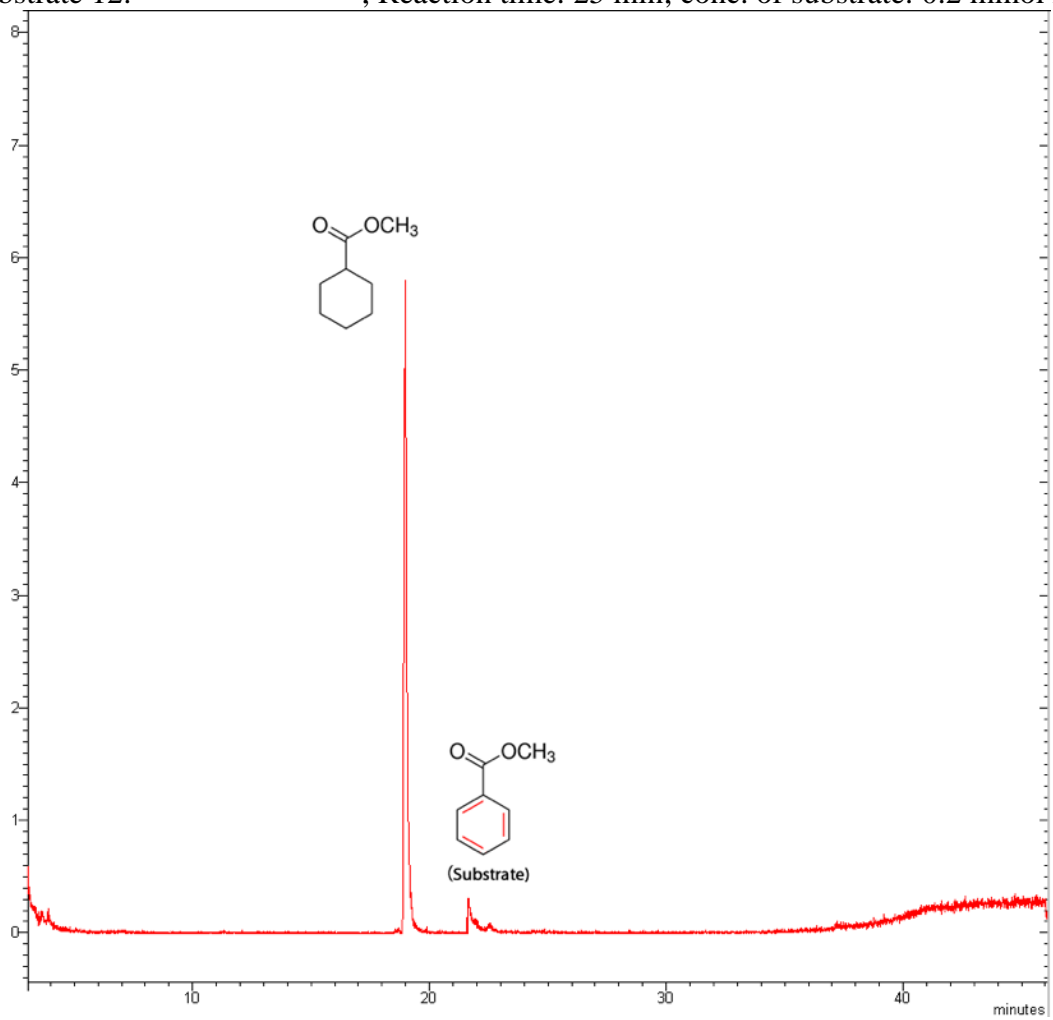
Substrate 10: CC=Cc1ccc(O)c(OC)c1; Reaction time: 8.3 min; conc. of substrate: 0.2 mmol l⁻¹



Substrate 11: c1ccc(cc1)C(=O)O; Reaction time: 20 min; conc. of substrate: 0.2 mmol l⁻¹



Substrate 12: COC(=O)c1ccccc1; Reaction time: 25 min; conc. of substrate: 0.2 mmol l⁻¹



References:

1. B. Keita and L. Nadjó, *Journal of Electroanalytical Chemistry and Interfacial Electrochemistry*, 1987, **217**, 287-304.
2. N. Singh, Y. Song, O. Y. Gutiérrez, D. M. Camaioni, C. T. Campbell and J. A. Lercher, *ACS Catal.*, 2016, **6**, 7466-7470.
3. S. Huang, X. Wu, W. Chen, T. Wang, Y. Wu and G. He, *Green Chem.*, 2016, **18**, 2353-2362.
4. I. V. Kozhevnikov and K. I. Matveev, *Applied Catalysis*, 1983, **5**, 135-150.
5. I. V. Kozhevnikov, *Chem. Rev.*, 1998, **98**, 171-198.
6. I. V. Kozhevnikov and K. I. Matveev, *Russian Chemical Reviews*, 1982, **51**, 1075.
7. I. V. Kozhevnikov, *Russian Chemical Reviews*, 1987, **56**, 811-825.
8. M. Boudart, *Chem. Rev.*, 1995, **95**, 661-666.
9. K. Kunimori, T. Uchijima, M. Yamada, H. Matsumoto, T. Hattori and Y. Murakami, *Applied Catalysis*, 1982, **4**, 67-81.